Chapter 1

General Introduction

Maternal mRNAs are actively transcribed and stored throughout oocyte growth in mammals. In fully grown oocytes, germinal vesicle break down (GVBD) is caused by a surge in luteinizing hormone from the pituitary, and then transcription ceases. Therefore, oocyte maturation, fertilization, and early embryonic development occur in the absence of gene transcription. In the absence of transcription, the embryonic cell sustains its protein production using stored mRNAs during oogenesis. This arrest in transcription continued until the resumption of gene expression after fertilization termed zygotic gene activation (ZGA). ZGA is the first transcription from the newly formed zygotic genome, which occurs between the middle 1-cell and the late 2-cell stages and is required for normal development in the mouse (Hamatani et al, 2004; Levey et al, 1977; Li et al, 2010; Minami et al, 2007; Schultz, 1993; Wang & Dey, 2006; Warner & Versteegh, 1974). The development of one-cell embryos treated with α-amanitin, an RNA polymerase II inhibitor, is arrested at the 2-cell stage because ZGA is suppressed (Levey et al, 1977; Warner & Versteegh, 1974). The second transcriptional event is mid-preimplantation gene activation (MGA), which occurs between the 4-cell and 8-cell stages in the mouse. During this period, genes required for cell fate specification, e.g., the transcription factors *Oct4* (also known as *Pou5f1*) and *Cdx2*, are expressed; these genes are known to be key regulators governing differentiation of the inner cell mass (ICM) and trophectoderm (TE) (Hamatani et al, 2004; Nichols et al, 1998; Niwa et al, 2005; Strumpf et al, 2005; Wang & Dey, 2006; Yoshikawa et al, 2006). However, the mechanisms of gene regulation at ZGA and MGA have not yet been clarified.

In general, gene expression is regulated through the transition of several epigenetic factors,

including transcription factors, chromatin-remodeling factors, and some enzymes. It has been reported that dynamic changes occur in chromatin structure during preimplantation development in mammals (Abdalla et al, 2009; Albert & Helin, 2010; Burton & Torres-Padilla, 2010; Corry et al, 2009; Morgan et al, 2005; Rasmussen & Corry, 2010; Shi & Wu, 2009). Histone post-translational modifications are introduced in a variety of ways. Several enzymes contribute to histone methylation (Zhang & Reinberg, 2001), acetylation (Sterner & Berger, 2000), phosphorylation (Nowak & Corces, 2004), and ubiquitination (Shilatifard, 2006). With respect to methylation, modifications of lysines 4, 36, and 79 of histone H3 (referred to as H3K4, H3K36, and H3K79, respectively) are associated with transcriptional activation, whereas modifications of lysines 9 and 27 of histone H3 and lysine 20 of histone H4 (referred to as H3K9, H3K27, and H4K20, respectively) are associated with transcriptional repression (Lepikhov & Walter, 2004; Sarmento et al, 2004). Especially, it has been reported that the levels of trimethylated H3K4 (H3K4me3) are gradually increased throughout oocyte growth and kept the high levels until ZGA in maternal chromosomes of one-cell embryo (Kageyama et al, 2007), while they are dramatically increased by ZGA in paternal chromosomes of the embryo (Albert & Peters, 2009; Lepikhov & Walter, 2004). Additionally, a previous study shows that in oocytes lacking functional *Mll2*, an H3K4 methyltransferase, chromosomes are misaligned, and maturation is arrested due to the decreased levels of H3K4me2/3, and most embryos lacking maternal *Mll2* are arrested between the 1- to 4-cell stages due to the decreased levels of H3K4me2/3 at ZGA (Andreu-Vieyra et al, 2010a), suggesting that the levels of H3K4me3 are important during oocyte maturation and ZGA. However, the molecular mechanisms of H3K4me3 during oocyte maturation and ZGA are unknown. In this study, we investigated the roles of epigenetic factors involved in H3K4me3.

Chapter 2

ING3 is essential for asymmetric cell division during mouse oocyte maturation

Abstract

ING3 (inhibitor of growth family, member 3) is a subunit of the nucleosome acetyltransferase of histone 4 (NuA4) complex, which activates gene expression. ING3, which contains a plant homeodomain (PHD) motif that can bind to trimethylated lysine 4 on histone H3 (H3K4me3), is ubiquitously expressed in mammalian tissues and governs transcriptional regulation, cell cycle control, and apoptosis via p53-mediated transcription or the Fas/caspase-8 pathway. Thus, ING3 plays a number of important roles in various somatic cells. However, the role(s) of ING3 in germ cells remains unknown. Here, we show that loss of ING3 function led to the failure of asymmetric cell division and cortical reorganization in the mouse oocyte. Immunostaining showed that in fully grown germinal vesicle (GV) oocytes, ING3 localized predominantly in the GV. After germinal vesicle breakdown (GVBD), ING3 homogeneously localized in the cytoplasm. In oocytes where *Ing3* was targeted by siRNA microinjection, we observed symmetric cell division during mouse oocyte maturation. In those oocytes, oocyte polarization was not established due to the failure to form an actin cap or a cortical granule-free domain (CGFD), the lack of which inhibited spindle migration. These features were among the main causes of abnormal symmetric cell division. Interestingly, an analysis of the mRNA expression levels of genes related to asymmetric cell division revealed that only *mTOR* was downregulated, and, furthermore, that genes downstream of mTOR (*e.g.*, *Cdc42*, *Rac1*, and *RhoA*) were also downregulated in si*Ing3*-injected oocytes. Therefore, ING3 may regulate asymmetric cell division through the *mTOR* pathway during mouse oocyte maturation.

Introduction

Oocyte maturation in mammals is characterized by a unique asymmetric cell division. After germinal vesicle breakdown (GVBD), the centrally positioned spindle migrates to the oocyte cortex; thereafter, asymmetric cell division occurs. Accordingly, the oocyte is transformed into a highly polarized, large metaphase II (MII)-arrested oocyte with an extruded small polar body (Maro & Verlhac, 2002). Failure of this asymmetric cell division to occur is usually observed in low quality oocytes or those that have experienced post-ovulatory aging, a cause of mammalian infertility (Miao et al, 2009; Webb et al, 1986). Asymmetric cell division depends upon the position of the spindle that is formed after GVBD. In a normal mouse oocyte, the germinal vesicle (GV) exists in the proximity of the central area of the oocyte (Alexandre & Mulnard, 1988), so that the spindle is formed near the center of the oocyte just after GVBD. Normal asymmetric cell division is induced after the spindle migrates to the oocyte cortex during meiotic maturation. It has been reported that spindle migration depends upon oocyte polarization, *e.g.*, the formation of an actin cap, where microfilaments are enriched, and a cortical granule free domain (CGFD), where cortical granules (CGs) are redistributed (Azoury et al, 2009; Deng et al, 2003; Longo & Chen, 1985; Sun & Schatten, 2006; Van Blerkom & Bell, 1986). However, details of the molecular mechanisms underlying oocyte polarization are poorly understood.

During oocyte growth in the mouse, dynamic changes occur in chromatin structure and histone modifications. With respect to histones H3 and H4, the levels of methylated (H3K4) and acetylated lysine residues (H3K9, H3K18, H4K5, and H4K12), which are associated with active gene expression, increase during mouse oogenesis and peak in fully grown GV oocytes (Kageyama et al, 2007). A previous study showed that deficiency of *Mll2*, a H3K4 methyltransferase, in mouse

oocytes causes anovulation and oocyte death (Andreu-Vieyra et al, 2010b). In *Mll2*-deficient oocytes, the levels of di- and trimethylated H3K4 (H3K4me2/3) are decreased, and abnormal maturation and aberrant gene expression, especially in apoptosis-related genes, are observed (Andreu-Vieyra et al, 2010b). These results suggest that the levels of H3K4me2/3 in oocytes are important for mouse oocyte maturation. ING (inhibition of growth) family members contain a plant homeodomain (PHD) motif through which the proteins can bind to H3K4me3, and are highly conserved from yeast to humans (He et al, 2005). ING family proteins have been found as subunits of chromatin remodeling complexes (Doyon et al, 2006), and are involved in transcriptional regulation, DNA repair, tumorigenesis, apoptosis, cellular senescence, and cell cycle arrest (Aguissa-Toure et al, 2011; Jafarnejad & Li, 2012). ING3 is an important subunit of the human NuA4 histone acetyltransferase complex (Doyon & Cote, 2004). ING3 is a tumor suppressor in melanoma and head and neck squamous cell carcinoma (HNSCC), and is involved in the regulation of p53-mediated transcription, cell cycle control, and apoptosis (Coles & Jones, 2009; Lu et al, 2012; Nagashima et al, 2003). Previous studies have demonstrated that overexpression of *ING3* in the human colorectal cancer cell line, RKO, suppresses cell growth through cell cycle control and induces apoptosis in a p53-dependent manner; however, no direct interactions between ING3 and p53 have been confirmed by co-immunoprecipitation (Nagashima et al, 2003). In melanoma cells, the overexpression of *ING3* induced *FAS* expression and promoted UV-induced apoptosis through a FAS/CASPASE-8-dependent pathway in a p53-independent manner (Wang & Li, 2006). Although *ING3* is ubiquitously expressed in mammalian tissues, it has been reported that *ING3* is more highly expressed in mouse, rhesus monkey, and human oocytes (Awe & Byrne, 2013). However, the role(s) of ING3 in oocytes is unknown.

In the present study, we investigated whether ING3 functions during mouse oocyte maturation. We found that the loss of ING3 function after siRNA treatment inhibited actin cap and CGFD formation, as well as oocyte polarization, leading to symmetric cell division. Since ING3 is involved in transcriptional regulation (Aguissa-Toure et al, 2011; Jafarnejad & Li, 2012), we also investigated whether ING3 regulated genes involved in asymmetric cell division during oocyte maturation. Interestingly, we found that among several asymmetric cell division–related genes, only *mTOR* expression was downregulated. Furthermore, mTOR's downstream genes, the Rho-family small GTPases (*e.g.*, *Cdc42*, *Rac1*, and *RhoA*) were also downregulated in oocytes after siRNA injection. It has also been reported that GTPases, including Cdc42, Rac1, and RhoA, can activate actin polymerization (Iden & Collard, 2008; Jordan & Canman, 2012; Wullschleger et al, 2006). Given these results, we propose that ING3 plays an important role in governing asymmetric cell division during mouse oocyte maturation by regulating actin polymerization via the *mTOR* pathway.

Materials and Methods

Oocyte collection and culture

Fully grown GV oocytes were collected from the ovaries of 8- to 10-week-old ICR mice (SLC, Shizuoka, Japan) in M2 medium (Table 1) containing 5.0 μM Milrinone (138-13801, Wako Pure Chemical Industries, Osaka, Japan). Milrinone, which increases cAMP, was used to inhibit GVBD. For maturation, oocytes were washed and cultured in M16 medium (Table 1) containing 4 mg/ml BSA (A311, Sigma-Aldrich, St. Louis, MO) under mineral oil (Sigma-Aldrich) at 37°C, in an atmosphere of 5% CO_2 in air.

Immunofluorescent staining

Oocytes were collected for immunofluorescent staining after 0, 2, 8, 9.5, or 12 h in culture, at which point most of the oocytes had reached the fully grown GV, GVBD, MI, ATI, or MII stages, respectively. For α-tubulin and actin staining, oocytes were fixed in 4% paraformaldehyde (Sigma-Aldrich) in Phosphate Buffered Saline (PBS) for 30 min at room temperature (RT). After washing three times in PBS containing 0.3% polyvinylpirrolidone (PVP K-30, Nacalai Tesque, Kyoto, Japan; PBS/PVP), oocytes were treated with 0.5% Triton X-100 (Sigma-Aldrich) in PBS for 40 min at RT, blocked in PBS containing 1.0% BSA (A9647, Sigma-Aldrich; blocking solution) for 1 h at RT and incubated overnight at 4°C with a FITC-conjugated anti-α-tubulin antibody (1:200 dilution; F2168, Sigma-Aldrich) or 2 μg/ml TRITC-conjugated phalloidin (P1951, Sigma-Aldrich) in blocking solution. For staining of ING3, cortical granules (CGs), acetylated H4K12 (AcH4K12), and mTOR, zona pellucidae were removed from the oocytes by acid Tyrode's solution (pH 2.5) (Table 2) and oocytes were fixed in PBS containing 4% paraformaldehyde for 20 min at 4°C. After washing three times in PBS/PVP, oocytes were treated with 0.5% Triton X-100 in PBS for 40 min

at RT, blocked in blocking solution for 1 h at RT, and incubated overnight at 4°C with one of the following reagents diluted into blocking solution: mouse anti-ING3 antibody (1:100 dilution, sc-101245, Santa Cruz Biotechnology Inc., Dallas, TX); 2 μg/ml FITC-conjugated lectin (L7381, Sigma-Aldrich); rabbit anti-AcH4K12 antibody (1:300 dilution 06-761, Millipore Corp., Billerica, MA); or rabbit anti-mTOR antibody (1:2000 dilution, ab2732, Abcam Ltd., Cambridge, UK). For ING3, AcH4K12, and mTOR staining, oocytes were washed three times in blocking solution and then incubated in blocking solution containing the secondary antibody (Alexa Fluor 488–conjugated goat anti-mouse IgG, 1:500 dilution, Invitrogen, Carlsbad, CA; Alexa Fluor 594–conjugated goat anti-rabbit IgG, 1:500 dilution, Invitrogen; or Alexa Fluor 488–conjugated goat anti-rabbit IgG, 1:500 dilution, Invitrogen) for 1 h at RT. After staining of α-tubulin, actin, ING3, CGs, AcH4K12, and mTOR, oocytes were washed three times in blocking solution for 15 min and nuclei were stained in PBS containing 10 μg/ml Hoechst 33342 (Sigma-Aldrich) for 10 min. After immunofluorescent staining, oocytes were mounted on slides in 50% glycerol/PBS and fluorescent signals were detected using a fluorescence microscope (BX50, Olympus, Tokyo, Japan). At least 20 oocytes were examined for each group.

Triton treatment of oocytes prior to PFA fixation

Triton treatment prior to PFA fixation was performed in order to examine whether protein was bound to chromatin (Hatanaka et al, 2013; Nakamura et al, 2012). Oocytes were treated with 0.2% Triton X-100 in PBS for 30 s. Then, they were washed with PBS three times and fixed in 4% PFA for 5 min at RT. After washing with PBS, immunofluorescent staining was performed as described above.

***Ing3* siRNA injection**

Approximately 5-10 pl of 50 μM *Ing3* siRNA (si*Ing3*; RNAi Inc., Japan, 5'-GGAUGAGAGGCGUUUACGUGC-3') in annealing buffer consisting of 30 mM HEPES-KOH (pH 7.4), 100 mM KOAc and 2 mM $Mg(OAc)_2$ was microinjected into the cytoplasm of a fully grown GV oocyte. The same amount of negative control siRNA (siControl; RNAi Inc.), which contains scrambled sequences from the si*Ing3* construct, was also microinjected as a control. After injection, the oocytes were cultured in M16 medium containing 5.0 μM Milrinone and 4 mg/ml BSA for 15.5 h, and then washed five times in fresh M16 medium containing 4 mg/ml BSA. Then, the oocytes were transferred to fresh M16 medium containing 4 mg/ml BSA and cultured under mineral oil at 37°C in an atmosphere of 5% CO_2 in air or harvested for quantitative RT-PCR (qRT-PCR) or immunoblotting.

RNA extraction and qRT-PCR

Total RNA from 50 fully grown GV oocytes was extracted using the TRIzol reagent (Invitrogen). RNase-free DNase I (Roche Diagnostics Corp., Indianapolis, IN) was added to the preparations to avoid genomic DNA contamination. For reverse transcription, Rever Tra Ace (Toyobo Co., Ltd., Osaka, Japan) and Oligo dT primer (Invitrogen) were used, according to the manufacturer's instructions. qPCR was carried out with THUNDERBIRD qPCR Mix (Toyobo Co., Ltd.) using Rotor-Gene 6000 (Qiagen, Hilden, Germany). Transcription levels were determined three times and normalized to *Gapdh*; relative gene expression was analyzed using the $2^{-\Delta\Delta Ct}$ method (Livak & Schmittgen, 2001). All primers used for PCR are listed in Table 3.

Immunoblotting

Fifty fully grown GV oocytes were collected in SDS sample buffer and boiled at 95°C for 4 min. The samples were kept at -80°C until use. Total protein was separated by 12.5%

SDS-polyacrylamide gel electrophoresis (SDS-PAGE) for 90 min at 20 mA and electrophoretically transferred to a polyvinylidene fluoride (PVDF) membrane (Immobilon-P, Millipore, Bedford, MA) over 2 h at 50 V. After three washes in Tris buffered saline (TBS) containing 0.1% Tween-20 (TBST), the membrane was blocked in TBST containing 5% skim milk for 1 h, and then incubated with either a mouse anti-ING3 antibody (1:200 dilution) or a mouse anti-α-tubulin antibody (1:5000 dilution; T9026; Sigma-Aldrich) in TBST containing 2% skim milk overnight at 4°C. After three washes in TBST, the membrane was incubated with an HRP-conjugated anti-mouse secondary antibody (1:2000 or 1:10000 dilution; GE Healthcare UK Ltd, Amersham, UK) in TBST for 1 h at RT. The membrane was extensively washed three times with TBST, and then processed with the Enhanced Chemilumidescence (ECL) detection system (GE Healthcare UK Ltd). α-tubulin was detected as an internal control.

Ethical approval for the use of animals

All animal experiments were approved by the Animal Research Committee of Kyoto University (Permit Number: 24-17) and were performed in accordance with the committee's guidelines.

Statistical analysis

Each experiment was repeated at least three times. The values were analyzed using a *t*-test. p values < 0.05 were considered to be statistically significant.

Table 1. Composition of M2 and M16 medium

Components	Amount	
	M2	M16
NaCl	553.3 mg/100 ml	553.3 mg/100 ml
KCl	35.6	35.6
$CaCl_2$·2H2O	25.2	25.2
KH_2PO_4	16.2	16.2
$MgSO_4$ · $7H_2O$	29.3	29.3
$NaHCO_3$	34.9	210.1
Glucose	100	100
HEPES	496.9	—
Na-pyruvate	0.4	0.4
Na Lactate (60% syrup)	434.9	434.9
Streptomycin	5	5
Penicillin G	6	6
BSA	4 mg/ ml	4 mg/ ml

Table 2. Composition of Acid Tyrode's Solution (pH 2.5)

Components	Amount
NaCl	800 mg/100 ml
KCl	20
$CaCl_2$	15
$MgCl_2 \cdot 6H_2O$	10
Na_2HPO_4	4
Glucose	100
PVP	400

Table 3. Primers used for qRT-PCR

Genes	GenBank Accession No.	Forward	Reverse
Ing3	NM_023626.4	ttcacatactcccgtggaaaa	gcgcttcagatttgaatttctt
Arpc3	NM_019824.3	gaaggaaatgtacacgctaggaa	gaggtacgcacgcatcatc
JMY	NM_021310.3	ttcaaattacaagccgtgcacccg	agctgccttctggacctttactga
mTOR	NM_020009.2	cttggagaaccagcccataa	ctggtttcaccaaaccgtct
ARF1	NM_001130408.1	Atgcgcattctcatggtg	aacagtctccacattgaaacca
Hsp90α	NM_010480.5	ggagataaatcctgatcactcca	caagatgaccagatccttcaca
Fmn2	NM_019445.2	gagacccttcaagctctctatga	gaagatcgactgtgcttttcaa
Mos	NM_020021.2	aagggaaaggaactgggatg	aacagccagggaagtttgg
Whamm	NM_001004185.3	cagccatttagagacatgcgagaa	ctaggacccagctcatcctcatc
Cdc42	NM_001243769.1	ttgttggtgatggtgctgtt	aatcctcttgccctgcagta
Rac1	NM_009007.2	agatgcaggccatcaagtgt	gagcaggcaggttttaccaa
RhoA	NM_016802.4	acaactgcatcccagaacct	taccacaagctccatcacca

Results

Localization of ING3 during oocyte maturation in the mouse

To investigate the role(s) of ING3 during mouse oocyte maturation, ING3 localization was initially examined at different stages of meiotic maturation. In the fully grown GV oocyte, ING3 was localized in GV. After GVBD, ING3 was dispersed homogenously into the cytoplasm (Fig. 1A). Furthermore, ING3 bound to the chromatin in fully grown GV oocytes (Fig. 1B).

Loss of ING3 function leads to spindle migration failure and the formation of a large polar body

The results of qRT-PCR and immunoblotting showed that the amount of *Ing3* mRNA and protein was dramatically decreased in si*Ing3*-injected oocytes (Fig. 2, A and B). After maturation in culture, si*Ing3*-injected oocytes exhibited symmetric cell division, showing 2-cell-like MII oocytes. Furthermore, the rate of symmetric cell division was significantly higher than that observed in siControl-injected oocytes. However, polar body (PB) extrusion was observed in most of the population (Fig. 2C–E). To analyze the phenotype of si*ing3*-injected oocytes, spindle migration was confirmed by immunostaining of α-tubulin. After 9.5 h in culture, the spindles moved to the cortex of the oocytes in siControl-injected oocytes, but remained centrally located in si*Ing3*-injected oocytes (Fig. 3, A and B). Moreover, the rate of symmetric cell division was dramatically increased at the end of the first meiosis in si*Ing3*-injected oocytes (Fig. 3C).

Loss of ING3 function abrogates cortical reorganization

Since spindle migration and asymmetric cell division are intimately related to oocyte polarity, the formation of the actin cap and CGFD, predominant features of oocyte polarization, was examined. As shown in Fig. 4A, in siControl-injected oocytes the chromosomes had already moved

to the cortical layer, the site of actin cap formation, by the MI stage after 9.5 h in culture, and at the ATI stage, the chromosomes dissociated at the region of the cortex with the actin cap. By the MII stage, a small PB and a large MII oocyte had formed and the chromosomes were located under the region of the cortex where the actin cap formed. By contrast, in si*Ing3*-injected oocytes, the chromosomes had not moved from the center of the cytoplasm and no actin cap was observed at the MI stage after 9.5 h in culture, and at the ATI stage, the chromosomes dissociated around the center of the cytoplasm. By the MII stage, an MII oocyte formed a 2-cell-like structure with no actin cap. As shown in Fig. 4B, in siControl-injected oocytes, CGs were lacking near the cortical layer where the chromosomes were located at the MI and MII stages, whereas in si*Ing3*-injected oocytes the chromosomes had not moved from the center of the cytoplasm and CGs were widely distributed through the cortical layer at the MI stage and were intensely localized in the cell adhesion region at the MII stage.

ING3 regulates *mTOR* expression in GV oocytes

The proportion of AcH4K12 that is acetylated by the NuA4 histone acetyltransferase complex (Doyon et al, 2006) in the fully grown GV oocyte was confirmed by immunofluorescent staining . In si*Ing3*-injected oocytes, the levels of AcH4K12 were decreased (Fig. 5A). To investigate the influence of this reduction in AcH4K12 levels in fully grown GV oocytes, the expression levels of the genes involved in asymmetric cell division were examined. In si*Ing3*-injected oocytes, the expression of *mTOR* was significantly downregulated as compared with the expression of *Arpc3, JMY, ARF1*, *Hsp90α*, *Fmn2*, *Mos*, or *Whamm* (Fig. 5B). Furthermore, immunostaining and qRT-PCR data showed that mTOR protein levels and mRNA levels of Rho-family GTPases, such as *Cdc42*, *Rac1*, and *RhoA*, were also decreased in si*Ing3*-injected

oocytes (Fig. 5, C and D).

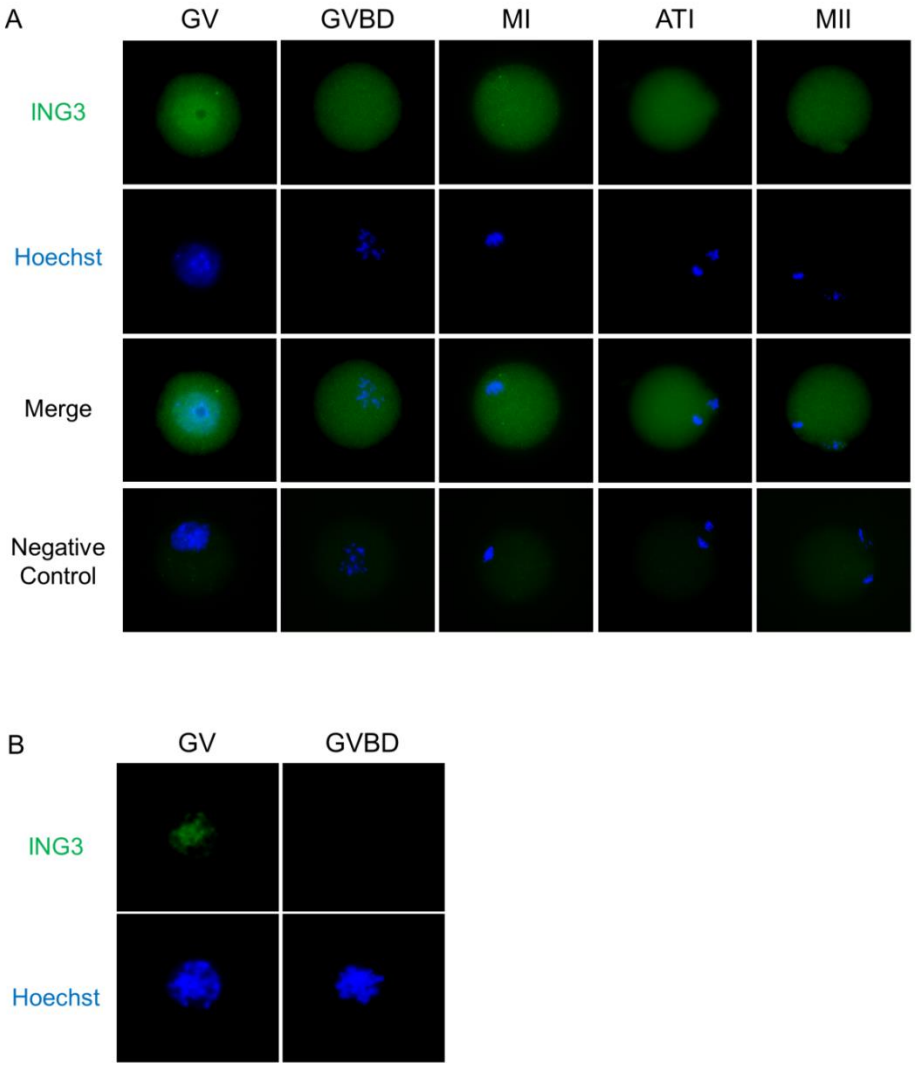

Figure 1. Localization of ING3 during mouse oocyte maturation.

(A) ING3 was predominantly localized in the nucleus in fully grown GV oocytes. After GVBD, ING3 localized homogeneously throughout the cytoplasm. Green, ING3; blue, chromatin. (B) ING3 bound to the chromatin in fully grown GV oocytes. Green, ING3; blue, chromatin.

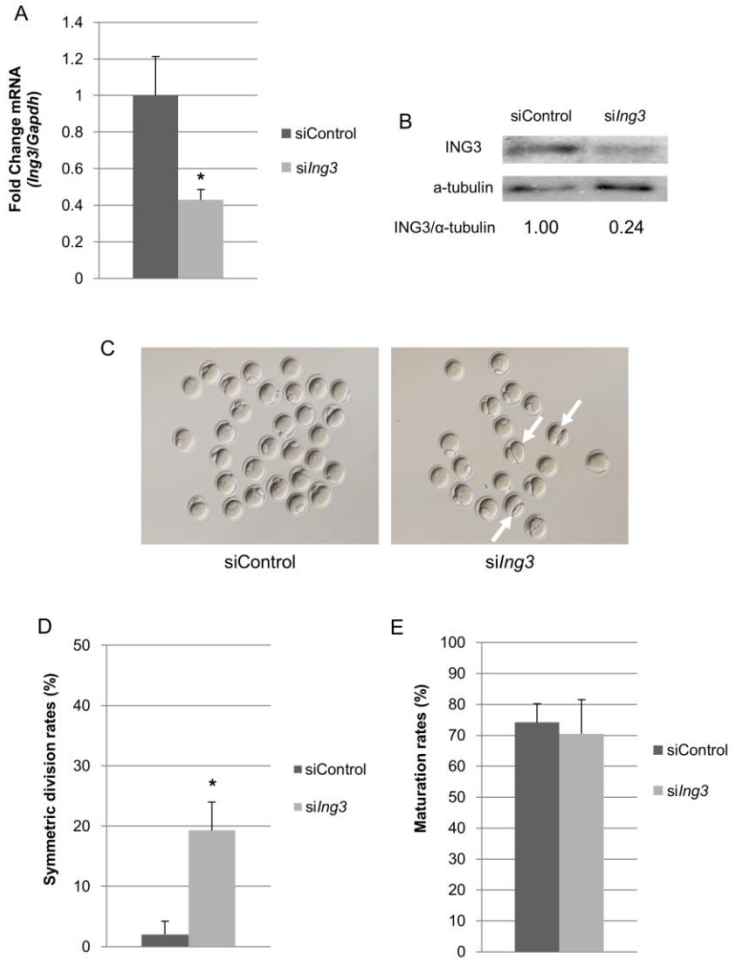

Figure 2. Effects of si*Ing3* injection on asymmetric cell division in mouse oocytes.

(A) *Ing3* mRNA was significantly decreased in the fully grown GV oocytes injected with si*Ing3* (**p* < 0.05). (B) ING3 protein levels, after normalization to α-tubulin, were decreased in fully grown GV oocytes injected with si*Ing3*. (C) Abnormal cell division was observed in several si*Ing3*-injected oocytes at the MII stage (arrows). (D) In si*Ing3*-injected oocytes, the rate of symmetric division was significantly increased as compared to that observed in siControl-injected oocytes (**p* < 0.05). (E) Maturation rates were not different between si*Ing3*- and siControl-injected oocytes.

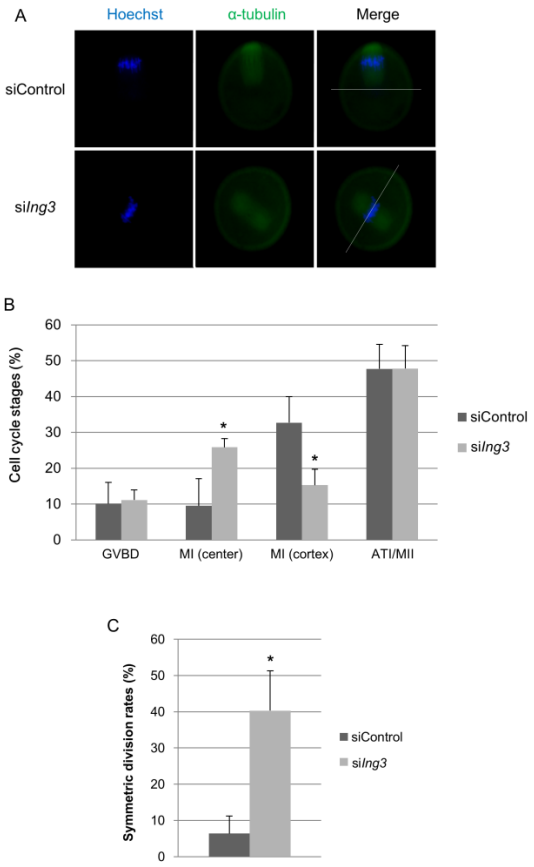

Figure 3. Effects of si*Ing3* injection on spindle migration in mouse oocytes.

(A) In siControl-injected oocytes, the spindle is located near the cortex at the MI stage after 9.5 h in culture. By contrast, in si*Ing3*-injected oocytes, the spindle is located at the center of the oocyte at the MI stage after 9.5 h in culture. Bars indicate the central position of the oocyte. Green, α-tubulin; blue, chromatin. (B) In siControl-injected oocytes, the frequency of spindles located at the cortex was significantly increased. By contrast, in si*Ing3*-injected oocytes, the frequency of spindles located at the center of the oocytes was significantly increased (*$p < 0.05$). The oocytes that were extruding or had extruded a polar body were considered to be at the ATI or MII (ATI/MII) stage. (C) In si*Ing3*-injected oocytes, the rate of symmetric division was significantly increased at the ATI/MII stages (*$p < 0.05$).

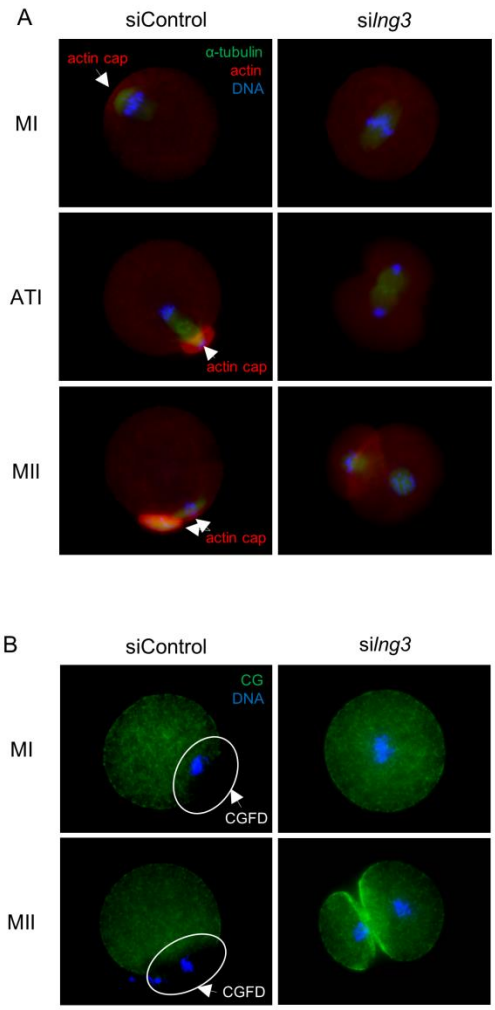

Figure 4. Effects of si*Ing3* injection on cortical reorganization in mouse oocytes.

(A) Actin cap formation was noted in siControl-injected oocytes at the MI, ATI, and MII stages. By contrast, no actin cap was formed in si*Ing3*-injected oocytes at any stage. Arrows indicate the actin cap. Green, α-tubulin; red, actin; blue, chromatin. (B) CGs were absent in the cortex where the chromosomes were located at the MI and MII stages in siControl-injected oocytes. By contrast, in si*Ing3*-injected oocytes, CGs were distributed throughout the cortex at the MI and MII stages, and were intensely localized in the region of cell adhesion at the MII stage. Circles and arrows denote the CGFD. Green, cortical granules; blue, chromatin.

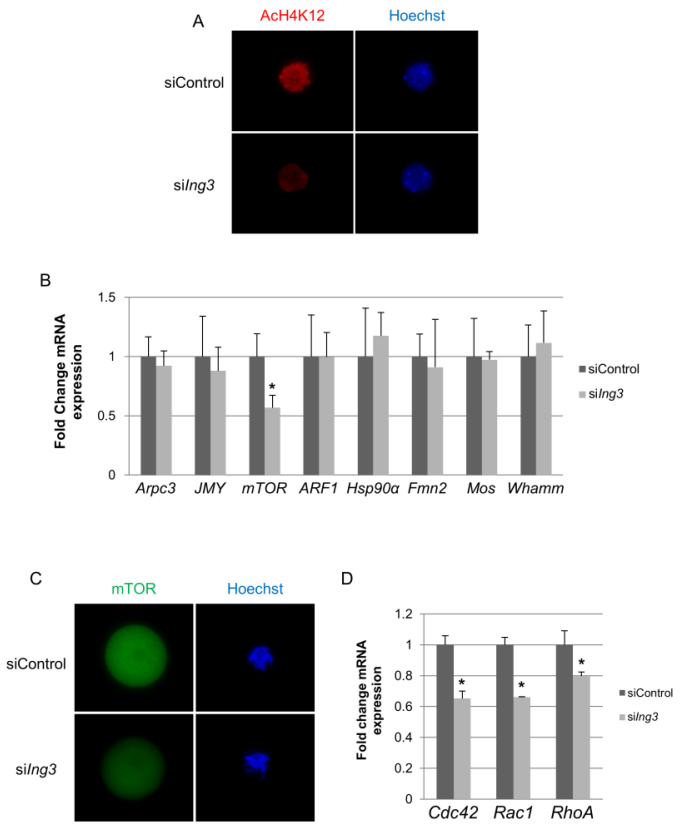

Figure 5. Effects of si*Ing3* injection on the levels of AcH4K12, asymmetric cell division–related gene expression, and mTOR protein in mouse oocytes.

(A) The levels of AcH4K12 in fully grown GV oocytes cultured for 15.5 h after injection of si*Ing3* were significantly decreased as compared to controls. Red, AcH4K12; blue, chromatin. (B) *mTOR* mRNA levels were significantly decreased after si*Ing3* injection in fully grown GV oocytes (*$p < 0.05$) as compared with other asymmetric cell division–related genes. (C) Although the protein localization of mTOR was not changed, the amount of mTOR protein was reduced in si*Ing3*-injected oocytes. Green, mTOR; blue, chromatin. (D) The expression levels of mTOR-downstream genes, such as *Cdc42*, *Rac1*, and *RhoA*, in fully grown GV oocytes were significantly decreased 15.5 h after si*Ing3* injection (*$p < 0.05$).

Discussion

ING3, which is an important subunit of the human NuA4 histone acetyltransferase complex and can recognize H3K4me3, is mainly known as a tumor suppressor gene. ING family proteins are involved in chromatin remodeling and regulate transcription (Aguissa-Toure et al, 2011). ING3 activates p53-transactivated promoters and modulates p53-mediated transcription, cell cycle control, and apoptosis (Nagashima et al, 2003). Here, we observed the subcellular localization of ING3 at different stages of meiotic maturation and the binding of ING3 to the chromatin in fully grown GV oocytes. Together with the knowledge that ING3 is an important subunit of the NuA4 histone acetyltransferase complex, these observations suggested that ING3 functions as a chromatin remodeling factor in fully grown GV oocytes. We also found that loss of ING3 function led to symmetric cell division due to a failure in spindle migration. Asymmetric cell division depends on the position of the spindle that is formed after GVBD. The maintenance of a central spindle position leads to symmetric cell division, a feature observed in aging mouse oocytes (Miao et al, 2009; Sun et al, 2012; Webb et al, 1986). Spindle migration is mainly regulated by actin filaments during oocyte maturation (Azoury et al, 2009; Maro & Verlhac, 2002; Sun & Schatten, 2006), and therefore is blocked by the inhibition of actin polymerization. In oocytes treated with cytochalasin D, an inhibitor of actin polymerization, spindle migration does not occur (Kubiak et al, 1991). During mitosis of somatic cells, actin filaments are formed with polymerized actin and actin polymerization is regulated by the interaction of proteins called nucleation promoting factors (NPFs) with the Arp2/3 complex (Pollard, 2007). NPFs initially interact with an actin monomer and polymerize actins to induce the formation of unbranched actin filaments. NPFs, actin filaments, and an actin monomer cooperate to stimulate the inactive Arp2/3 complex to form actin filament

branches on the side of existing filaments (Fededa & Gerlich, 2012). During mouse oocyte maturation, Arp2/3 co-localizes with the actin cap. This subcellular localization is changed in oocytes treated with cytochalasin B, which is also an inhibitor of actin polymerization, and the loss of function of the *Arp2/3* complex causes symmetric cell division because the actin cap does not form where actin filaments are converged by phosphatidylinositol (3,4,5)-triphosphate (PtdIns(3,4,5)P3) (Sun et al, 2011b; Zheng et al, 2012). Together, these results suggest that actin polymerization is a key regulator of asymmetric cell division in the mouse. In addition, actin polymerization is also involved in oocyte polarization through formation of the actin cap. Oocyte polarization, as indicated by the formation of the actin cap and CGFD, is one of the most important processes underlying asymmetric cell division during oocyte maturation (Deng et al, 2003; Longo & Chen, 1985; Van Blerkom & Bell, 1986), and the disruption of oocyte polarization results in symmetric cell division (Lee et al, 2012; Metchat et al, 2009; Sun et al, 2011a; Sun et al, 2011b; Wang et al, 2009). Thus, the disruption of oocyte polarization in *Ing3*-inhibited oocytes abrogated spindle migration and led to symmetric cell division.

It has been reported that the loss of function of *Arp2/3*, *JMY*, *mTOR*, *ARF1*, *Hsp90α, GM130*, *Fmn2*, *Mos*, or *Whamm* during mouse oocyte maturation disrupts oocyte polarity, impedes spindle migration, and leads to symmetric cell division (Dumont et al, 2007; Huang et al, 2013; Lee et al, 2012; Metchat et al, 2009; Sun et al, 2011a; Sun et al, 2011b; Verlhac et al, 2000; Wang et al, 2009; Zhang et al, 2011). Since ING3 is an important subunit of the NuA4 histone acetyltransferase complex, which activates gene expression, and ING3 bound to the chromatin in the fully grown GV oocytes, it is possible that ING3 regulates some genes that are involved in asymmetric cell division during oocyte maturation through histone acetylation. Indeed, we found that ING3 regulated the

expression of *mTOR* and is involved in histone acetylation in fully grown GV oocytes, suggesting that ING3 regulates the expression of *mTOR* through histone acetylation. During mitosis in somatic cells, mTOR regulates actin polymerization by activating small GTPases (Cdc42, Rac1, and RhoA). In turn, activated small GTPases regulate the actin cytoskeleton and microtubule dynamics through the activation of NPFs (Iden & Collard, 2008; Wullschleger et al, 2006). Cdc42, Rac1, and RhoA cooperate temporally and spatially to regulate actin dynamics and have an influence on cellular processes including cell motility, cell polarization, cell adhesion, and cytokinesis (Jordan & Canman, 2012). During oocyte maturation, mTOR also regulates oocyte polarization through its involvement in actin cap formation via the activation of small GTPases. Therefore, loss of mTOR function leads to symmetric cell division (Lee et al, 2012). Thus, the observation that ING3 regulates the expression of *mTOR* and Rho-family small GTPases in fully grown GV oocytes suggests that ING3 plays important roles in actin polymerization via the *mTOR* pathway during mouse oocyte maturation.

Nonetheless, our results were slightly different from those obtained in mTOR inhibited oocytes. Namely, in mTOR-inhibited oocytes during mouse oocyte maturation cell cycle stages are delayed after 9.5 h in culture (Lee et al, 2012). By contrast, loss of ING3 function did not delay the progression of cell cycle stages over 9.5 h in culture; however, the rate of symmetric cell division in oocytes at the end of first meiosis was significantly increased. It is probable that cell cycle regulation by RhoA proteins (Zhong et al, 2005) was not sufficiently abrogated after microinjection of si*Ing3* in the fully grown GV oocytes despite the decrease observed in *RhoA* mRNA. This may explain the lack of notable effect on the cell cycle in these oocytes.

In eukaryotic cells, chromatin serves as a dynamic and active participant in multiple

nuclear processes, and plays a remarkable role in the regulation of gene expression. Many histone methyltransferases and chromatin remodeling factors have pivotal roles in biological processes during development and disease, *e.g.*, neurological disorders and cancer (Albert & Helin, 2010; Doyon & Cote, 2004). In addition, it has been reported that the levels of di- and trimethylated H3K4 in oocytes are important for maturation in the mouse (Andreu-Vieyra et al, 2010b; Ma & Schultz, 2013). In oocytes lacking functional *Mll2*, the levels of di- and trimethylated lysine are decreased, chromosomes are misaligned, and maturation is arrested (Andreu-Vieyra et al, 2010b), suggesting that histone methyltransferase is important for meiosis. However, the roles of genes that govern histone methylation during mouse oocyte maturation are poorly understood. It has been reported that ING3 is a member of the ING family of proteins that bind to H3K4me3, and that ING3 is an important subunit of the human NuA4 histone acetyltransferase complex (Doyon et al, 2006; Doyon & Cote, 2004; Mellor, 2006). The NuA4 histone acetyltransferase complex governs the acetylation of histones H4 and H2A (Doyon & Cote, 2004). In this study, we found that ING3 was involved in the asymmetric cell division of mouse oocytes during the first meiotic cell division, and that ING3 promoted H4K12 acetylation, suggesting that the chromatin remodeling factors involved in the recognition of methylated H3K4 also function during mouse oocyte maturation.

In conclusion, our results demonstrated that ING3 function is critical for maintaining asymmetric cell division, and indicated the possibility that an elucidation of the genes involved in chromatin remodeling may shed light on the molecular mechanisms of mouse oocyte maturation.

Chapter 3

Histone methyltransferase *Smyd3* regulates early embryonic lineage commitment through mid-preimplantation gene activation in the mouse

Abstract

Smyd3 (SET and MYND domain–containing protein 3) is a histone H3 lysine 4 di- and tri-methyltransferase that forms a transcriptional complex with RNA polymerase II and activates the transcription of oncogenes and cell cycle genes in human cancer cells. However, the study of *Smyd3* in mammalian early embryonic development has not yet been addressed. In this study, we investigated the expression pattern of *Smyd3* in mouse preimplantation embryos and the effects of RNA interference (RNAi)-mediated *Smyd3* repression on the development of mouse embryos. Here, we showed that *Smyd3* mRNA levels increased after the 2-cell stage, peaked at the 4-cell stage, and gradually decreased thereafter. Moreover, in 2-cell to 8-cell embryos, SMYD3 staining was more intense in the nuclei than in the cytoplasm. In *Smyd3*-knockdown embryos, the percentage of inner cell mass (ICM)-derived colony formation and trophectoderm (TE)-derived cell attachment was significantly decreased, resulting in a reduction in the number of viable offspring. Furthermore, the expression of *Oct4* and *Cdx2* during mid-preimplantation gene activation was significantly decreased in *Smyd3*-knockdown embryos. In addition, the transcription levels of ICM and epiblast markers, such as *Oct4*, *Nanog*, and *Sox2*; of primitive endoderm markers, such as *Gata6*; and of TE markers, such as *Cdx2* and *Eomes*, were significantly decreased in *Smyd3*-knockdown blastocysts. These findings indicated that SMYD3 plays an important role in early embryonic lineage commitment and peri-implantation development through the activation of lineage-specific genes.

Introduction

Embryonic development in mammals is characterized by an initial preimplantation phase that serves to prepare the embryo for implantation. Transcription from the newly formed zygotic genome, known as zygotic gene activation (ZGA), begins after fertilization between the late 1-cell stage and the 2-cell stage (Latham & Schultz; Li et al; Schultz & Worrad). Subsequently, mid-preimplantation gene activation (MGA) occurs during the 4- to 8-cell stages (Hamatani et al). Both ZGA and MGA consist of new gene expression from the embryonic genome, and both steps require proper lineage commitment and differentiation. The first lineage differentiation gives rise to the inner cell mass (ICM) and trophectoderm (TE). The pluripotency of the ICM lineage is regulated by the transcription factors *Oct4* (also known as *Pou5f1*), *Nanog*, and *Sox2* (Avilion et al; Mitsui et al; Nichols et al), and the specification and differentiation of the TE lineage is regulated by the transcription factors *Cdx2* and *Eomes* (Russ et al; Strumpf et al). Prior to implantation, the ICM gives rise to the epiblast (EPI), which predominantly expresses *Nanog*, and the primitive endoderm (PE), which predominantly expresses *Gata6* (Chazaud et al; Rossant). The EPI will eventually give rise to the fetus, while the PE will develop into the visceral and parietal endoderm of the yolk sacs, and the TE will become the fetal placenta.

In general, gene expression is regulated through the transition of several epigenetic factors, including transcription factors, chromatin-remodeling factors, and some enzymes. Examples of epigenetic changes that take place during preimplantation development include DNA methylation, histone post-translational modifications, and histone variant exchange (Akiyama et al; Hirasawa et al; Santos et al; Sarmento et al). Drastic changes in many varieties of histone post-translational modifications occur during ZGA. Histone post-translational modifications are introduced in a variety of ways. Several enzymes contribute to histone

methylation (Zhang & Reinberg), acetylation (Sterner & Berger), phosphorylation (Nowak & Corces), and ubiquitination (Shilatifard). With respect to methylation, modifications of lysines 4, 36, and 79 of histone H3 (referred to as H3K4, H3K36, and H3K79, respectively) are associated with transcriptional activation, whereas modifications of lysines 9 and 27 of histone H3 and lysine 20 of histone H4 (referred to as H3K9, H3K27, and H4K20, respectively) are associated with transcriptional repression (Lepikhov & Walter; Sarmento et al). Except for the H3K79 methyltransferase, known as DOT1L, histone methyltransferases (HMTase) include a conserved catalytic domain called the SET domain (Feng et al, 2002; Zhang & Reinberg). *Smyd3* (SET and MYND domain containing protein 3) encodes a protein comprising 428 amino acids and containing a SET-domain, a MYND-type zinc finger domain, and a SET-N region. SMYD3 has been reported to be capable of methylating both H3K4 and H4K5 (Hamamoto et al; Van Aller et al). Evidence has accumulated that SMYD3 recruits RNA polymerase II through an RNA helicase to form a transcription complex, and that it elicits its oncogenic effects by activating the transcription of downstream target genes (Hamamoto et al; Hamamoto et al; Liu et al; Liu et al). Previous reports have demonstrated that enhanced expression of SMYD3 is essential for the growth of human cancer cells (Hamamoto et al; Hamamoto et al), whereas the suppression of SMYD3 expression leads to apoptosis and the inhibition of cell growth, migration, and invasion (Zou et al). Recent studies have determined that *Smyd3* plays an important role in the development of heart and skeletal muscle during zebrafish embryogenesis (Fujii et al). However, the role of SMYD3 in mammalian early embryonic development has not been previously addressed.

Here, we examined the expression pattern of *Smyd3* mRNA and the localization of SMYD3 protein in mouse preimplantation embryos, and found that siRNA-mediated knockdown of *Smyd3* during early stages of embryonic development suppressed *Oct4* and *Cdx2*

at MGA. Furthermore, *Smyd3* knockdown early in development reduced the blastocyst-stage expression of ICM/EPI markers, e.g., *Oct4*, *Nanog*, and *Sox2*; of PE markers, e.g., *Gata6*; and of TE markers, e.g., *Cdx2* and *Eomes*. From these results, we propose that SMYD3 plays an important role in early embryonic lineage commitment through the activation of lineage-specific genes.

Materials and Methods

In vitro fertilization and embryo culture

Female ICR mice (8-10-week-old, Japan SLC, Hamamatsu, Japan) were superovulated with an intraperitoneal injection of 5 IU equine chorionic gonadotropin (eCG, Asuka Pharmaceutical, Tokyo, Japan) followed 48 h later by an intraperitoneal injection of 5 IU human chorionic gonadotropin (hCG, Asuka Pharmaceutical). Ovulated oocytes (metaphase II-arrested oocytes) were collected 14 h after the hCG injection and placed in a 90-μL fertilization droplet of modified human tubal fluid (mHTF) medium (Table 4) supplemented with 4 mg/mL BSA (A3311, Sigma-Aldrich, St. Louis, MO). Spermatozoa were collected from the cauda epididymis of mature male mice and capacitated by preincubation for 2 h in mHTF medium. After preincubation, sperm were introduced into fertilization droplets at a final concentration of 1×10^6 cells/mL. Three hours after insemination, fertilized eggs were washed and cultured until embryonic day 5.5 (E5.5) in K-modified simplex optimized medium (KSOM) (Table 4) containing 4 mg/mL BSA under mineral oil (Sigma-Aldrich) at 37 ℃, in an atmosphere of 5% CO_2 in air or used for microinjection (Tsukamoto et al, 2013) and cultured until E5.5.

RNA extraction and quantitative RT-PCR (qRT-PCR)

Metaphase II oocytes, and 1-cell, 2-cell, 4-cell, 8-cell, morula, and blastocyst stage embryos were collected at 14, 28, 50, 62, 69, 90 and 122 h after hCG injection, respectively. RNA extraction and qRT-PCR were performed as described (Suzuki et al). Total RNA from 30 embryos at each stage was extracted using the TRIzol reagent (Invitrogen, Carlsbad, CA). RNase-free DNase I (Roche Diagnostics Corp., Indianapolis, IN) was added to the preparations to avoid genomic DNA contamination. For reverse transcription, ReverTra Ace (Toyobo Co., Ltd., Osaka, Japan) and Oligo dT primers (Invitrogen) were used according to the manufacturer’s instructions. qRT-PCR was carried out with the THUNDERBIRD qPCR Mix

(Toyobo Co., Ltd.) using a Rotor-Gene 6000 (Corbett Life Science, Sydney, Australia). Transcription levels were determined using three different sets of 30 embryos per stage and normalized to *H2afz* or *Gapdh*; relative gene expression was analyzed using the $2^{-\Delta\Delta Ct}$ method (Livak & Schmittgen, 2001). All primers used for PCR are listed in Table 5.

Microinjection of siRNA

Fertilized embryos transferred to KSOM were microinjected into the cytoplasm with 5–10 pL of 100 μM *Smyd3* siRNA (si*Smyd3*; RNAi Inc., Japan, 5'-GCAGGGUUAUCGUCAAGCUGA-3') between 3 and 4 h after insemination. The same amount of negative control siRNA (siControl; RNAi Inc.), which contains scrambled sequences from the si*Smyd3* construct, was also microinjected as a control. To examine the developmental competency and hatching ability, embryos were observed at 50 (E1.5), 74 (E2.5), 98 (E3.5), 122 (E4.5) and 146 h (E5.5) after hCG injection. After siRNA injection, embryos were harvested at either the 4- and 8-cell stages (62 and 69 h after hCG injection, respectively) for qRT-PCR and immunostaining, at the morula or blastocyst stage (98 h after hCG injection) for outgrowth experiments, or at the blastocyst stage (122 h after hCG injection) for qRT-PCR, immunostaining, and immunoblotting.

Outgrowth experiment and embryo transfer

Outgrowth experiments were performed using morula or blastocyst stage embryos collected 98 h after hCG injection as previously described (Yamada et al). After culture for 4 days, the percentage of blastocysts that underwent outgrowth was calculated and photographed. A portion of the embryos that reached the 2-cell stage after microinjection was transferred into the oviducts of 0.5 dpc pseudopregnant ICR female mice. These females were sacrificed at Day 19, and pups were counted. The experiment was repeated four times.

Immunostaining

Embryos for immunostaining were collected as described above. For SMYD3, trimethylated H3K4 (H3K4me3), and EOMES staining, embryos were fixed in 4% paraformaldehyde in PBS for 20 min at 4 °C after the removal of the zona pellucidae with Acid Tyrode's Solution (pH 2.5) (Table 2). After washing three times in PBS containing 0.3% polyvinylpyrrolidone (PVP K-30, Nacalai Tesque, Kyoto, Japan) (PBS/PVP), fixed embryos were treated with 0.5% Triton X-100 (Sigma-Aldrich) in PBS for 40 min at room temperature (RT), and blocked in PBS containing 1% BSA for 1h at RT (for SMYD3 and EOMES) or 3% BSA overnight at 4 °C (for H3K4me3). Next, embryos were incubated overnight at 4 °C with a rabbit anti-SMYD3 antibody (1:100 dilution, 10 μg/mL; ab16027, Abcam Ltd, Cambridge, UK) or rabbit anti-EOMES antibody (1:500 dilution, 0.4 μg/mL; ab23345, Abcam Ltd), or for 1 h at RT with a rabbit anti-H3K4me3 antibody (1:200 dilution, 2.5 μg/mL; ab8580, Abcam Ltd) in antibody dilution buffer (PBS containing 1% BSA). Embryos were washed three times in antibody dilution buffer, and then incubated with the appropriate secondary antibody diluted at 1:500 (Alexa Fluor 488-conjugated goat anti-rabbit IgG or Alexa Fluor 594-conjugated goat anti rabbit IgG, Invitrogen) for 1 h at RT. Immunostaining with normal rabbit IgG (sc-2027, Santa Cruz Biotechnology, Dallas, TX) was performed as a negative control for the specificity of the anti-SMYD3 antibody. For NANOG, SOX2, and GATA6 staining, embryos were fixed in 4% paraformaldehyde in PBS for 10 min at RT. After washing three times in PBS/PVP, fixed embryos were treated with 0.5% Triton X-100 (Sigma-Aldrich) in PBS for 30 min at RT, blocked in PBS containing 10% Fetal Bovine Serum and 0.1% Triton X-100 for 1 h at RT. Next, embryos were incubated overnight at 4 °C with a rabbit anti-NANOG antibody (1:1000 dilution, 1 μg/mL; ab5731, Millipore, Bedford, MA), a goat anti-SOX2 antibody (1:100 dilution, 2 μg/mL; sc-17320, Santa Cruz Biotechnology), or a goat anti-GATA6 antibody (1:1000 dilution, 0.2 μg/mL; AF1700, R & D systems, Inc., Minneapolis, MN) in blocking solution for overnight

at 4 °C. Embryos were washed three times in blocking solution, and then incubated with the appropriate secondary antibody diluted at 1:750 (Alexa Fluor 594-conjugated goat anti-rabbit IgG, Invitrogen) or 1:500 or 1:750 (Alexa Fluor 594-conjugated rabbit anti-goat IgG, Invitrogen) for 1 h at RT. After staining, the samples were washed three times in antibody dilution buffer or blocking solution for 15 min, and nuclei were stained in PBS containing 10 μg/mL Hoechst 33342 (Sigma-Aldrich) for 10 min at RT. Immunofluorescent staining for OCT4 and CDX2 was performed as previously described (Isaji et al). After staining, embryos were mounted on slides in 50% glycerol/PBS and SMYD3-related signals were observed using a fluorescence microscope (BZ-X700, Keyence, Osaka, Japan) equipped with structured illumination microscopy (Gustafsson, 2005; Hosny et al, 2013). Fluorescein signals related to OCT4, CDX2, H3K4me3, NANOG, SOX2, GATA6, and EOMES were detected using fluorescence microscopy (BX50, Olympus, Tokyo, Japan). At least 20 samples were examined in each group. The numbers of ICM and TE cells were determined by counting OCT4- and CDX2-positive cells, respectively. The total embryonic cell numbers were obtained by adding the numbers determined for the ICM and TE cells.

Immunoblotting

A hundred blastocysts were collected in SDS sample buffer/Lysis buffer (1:1) and incubated twice for 2 min at 95 °C. Total protein was separated by SDS-polyacrylamide gel electrophoresis (SDS-PAGE) on a 12.5% gel run for 90 min at 20 mA, followed by transfer to a polyvinylidene fluoride (PVDF) membrane (Immobilon-P, Millipore) over 2 h at 50 V. After three washes in Tris-buffered saline (TBS) containing 0.1% Tween-20 (TBS-T), the membrane was blocked for 1 h in TBS-T containing 5% skim milk, and then incubated overnight at 4 °C with one of the following reagents diluted in TBS-T containing 2% skim milk: a mouse anti-α-TUBULIN antibody (1:5000 dilution, 1.16 μg/mL; T9026; Sigma-Aldrich), a rabbit

anti-SMYD3 antibody (1:100 dilution, 10 μg/mL), a rabbit anti-H3K4me3 antibody (1:200 dilution, 2.5 μg/mL), a rabbit anti-OCT4 antibody (1:500 dilution, 400 ng/mL; C-10; sc-5279, Santa Cruz Biotechnology), or a mouse anti-CDX2 antibody (1:500 dilution, 100 μg/mL; CDX-88; BioGenex, San Ramon, CA). After three washes in TBS-T, the membrane was incubated with an HRP-conjugated anti-mouse secondary antibody (1:2000 or 1:10000 dilution; GE Healthcare UK Ltd, Little Chalfont, UK) or an HRP-conjugated anti-rabbit secondary antibody (1:1000 or 1:2000 dilution; GE Healthcare UK Ltd) in TBS-T for 1 h at RT. The membrane was extensively washed three times with TBS-T, and then bound antibodies were detected using the Enhanced Chemiluminescence (ECL) system (GE Healthcare UK Ltd). α-TUBULIN was used as an internal control.

Statistical Analysis

All data were expressed as the mean ± SEM. Statistical analysis of the date was performed by analysis of variance (ANOVA) with Student's t-test for comparing two groups.

Ethical Approval for the Use of Animals

All animal experiments were approved by the Animal Research Committee of Kyoto University (Permit Number: 24-17) and were performed in accordance with the committee's guidelines.

Table 4. Composition of mHTF and KSOM medium

Components	Amount			
	mHTF		KSOM	
NaCl	593.8	mg/100 ml	555.2	mg/100 ml
KCl	35.0		18.6	
$CaCl_2$	57.0		19.0	
KH_2PO_4	5.4		4.8	
$MgSO_4 \cdot 7H_2O$	4.9		4.9	
$NaHCO_3$	210.0		210.0	
Glucose	50.0		3.6	
L-Glutamine	—		14.6	
Na-pyruvate	3.7		2.2	
Na Lactate (60% syrup)	0.3	ml/100 ml	0.2	ml/100 ml
Streptomycin	5.0	mg/100 ml	5.0	mg/100 ml
Penicillin G	6.3		6.3	
EDTA・2Na (10 mM Solution)	—		100.0	μl/100ml
BSA	4.0	mg/ ml	1.0	mg/ ml
EAA	—		1.0	ml/100 ml
NEAA	—		500.0	μl/100ml

Table 5. Primers used for qRT-PCR

Genes	GeneBank Accession No.	Forward	Reverse
Smyd3	NM_027188.3	ggatctgaggtgtggatctga	ggttggcagtcgtgaacttt
Oct4	NM_001252452.1	atggggaaagaagctcagtg	caaaatgatgagtgacagacagg
Sox2	NM_011443.3	aaaccaccaatcccatcca	ccccaaaaagaagtcccaag
Nanog	NM_001289828.1	ttcttgcttacaagggtctgc	agaggaagggcgaggaga
Gata6	NM_010258.3	ggtctctacagcaagatgaatgg	tggcacaggacagtccaag
Cdx2	NM_007673.3	agctgctgtaggcggaatgtatg	tcagtgactcgaacagcagcaa
Eomes	NM_001164789.1	accggcaccaaactgaga	aagctcaagaaaggaaacatgc
Gapdh	NM_001289726.1	cgtgttcctacccccaatgt	tgtcatcatacttggcaggtttc
H2afz	NM_016750.3	tccagtggactgtatctctgtga	gactcgaatgcagaaatttgg

Results

Expression of the *Smyd3* mRNA and protein in mouse preimplantation embryos

First, we revealed the expression pattern of *Smyd3* mRNA and the localization of SMYD3 protein in mouse preimplantation embryos. qRT-PCR analysis of *Smyd3* mRNA in preimplantation embryos indicated that the expression levels increased after the 1-cell stage, peaked at the 4-cell stage, and then slightly decreased (Fig. 6A). Furthermore, immunostaining showed that SMYD3 localizes to the nuclei and cytoplasm from the 1-cell to the blastocyst stage. Especially, in 2- to 8-cell embryos, SMYD3 dominantly localizes to the nuclei (Fig. 6B).

Effects of *Smyd3* knockdown on the development of mouse embryos

In order to investigate the role of *Smyd3* in early embryonic development, we knocked down the expression of *Smyd3* in mouse preimplantation embryos. Embryos injected with siRNA targeting *Smyd3* (si*Smyd3*) were cultured until E5.5. qRT-PCR and immunoblotting showed that the reduction in the expression of *Smyd3* mRNA and protein continued through the blastocyst stage (Fig. 7, A and B). Additionally, Immunostaining showed that SMYD3 protein levels were also reduced from the 1-cell stage (Fig. 7C). Nevertheless, no differences between *Smyd3*-knockdown and control embryos were noted with respect to morphology or percentage of embryonic development up to E5.5 (Fig. 8, A and B). Cell numbers in E4.5 blastocysts were counted after OCT4 (ICM) and CDX2 (TE) staining. The data demonstrated that *Smyd3*-knockdown blastocysts had normal numbers of cells in both populations (Fig. 8C). To examine the pluripotency of *Smyd3*-knockdown embryos, outgrowth experiments were performed on E3.5 embryos. *Smyd3*-knockdown embryos formed limited outgrowths that were devoid of ICM-derived colonies and TE-derived cells (Fig. 9A). The percentages of successful attachment and ICM-derived colony formation in *Smyd3*-knockdown embryos were significantly reduced as compared to control embryos (Fig. 9B). Furthermore, to test the

viability of *Smyd3*-knockdown embryos in vivo, si*Smyd3*-injected embryos were transferred into the oviducts of pseudopregnant mice. The percentage of offspring derived from *Smyd3*-knockdown embryos was significantly reduced as compared to controls (Table 6).

Knockdown of *Smyd3* leads to the down-regulation of linage-specific genes

In order to analyze the reasons of the defect of peri-implantation embryonic development, we performed qRT-PCR on 4- and 8-cell stage embryos for *Smyd3* and early differentiation markers such as *Oct4* and *Cdx2*. In addition, to confirm the levels of H3K4me3 in *Smyd3*-knockdown embryos at the 4- and 8-cell stages immunostaining was performed. The results demonstrated that the expression of *Smyd3* mRNA was significantly decreased in *Smyd3*-knockdown embryos (Fig. 10A); however, H3K4me3 levels remained unchanged (Fig. 10B). Interestingly, the transcription of *Oct4* at the 4-cell and 8-cell stages and of *Cdx2* at the 8-cell stage was significantly decreased in *Smyd3*-knockdown embryos (Fig. 10, C and D). To further investigate the influence of the reduced expression of *Smyd3*, *Oct4*, and *Cdx2* at the 4- and 8-cell stages, we performed qRT-PCR on E4.5 blastocyst stage embryos for *H2afz*—an internal control—and lineage-specific genes, e.g., the ICM/EPI markers, *Oct4*, *Nanog*, and *Sox2*; the PE marker, *Gata6*; and the TE markers, *Cdx2* and *Eomes*. The results demonstrated that the transcription levels of *Oct4*, *Nanog*, *Sox2*, *Gata6*, *Cdx2*, and *Eomes* were all significantly decreased in *Smyd3*-knockdown embryos at the blastocyst stage, while *H2afz* transcript levels remained unchanged (Fig. 11A). Furthermore, the protein levels of OCT4, CDX2, NANOG, SOX2, GATA6, and EOMES were confirmed on E4.5 blastocysts. Consequently, the levels of OCT4, CDX2, NANOG, SOX2, GATA6, and EOMES were significantly reduced in *Smyd3*-knockdown embryos at the blastocyst stage (Fig. 11B, 12A). Additionally, global H3K4me3 levels also remained unchanged in the treated embryos at the blastocyst stage (Fig. 12B).

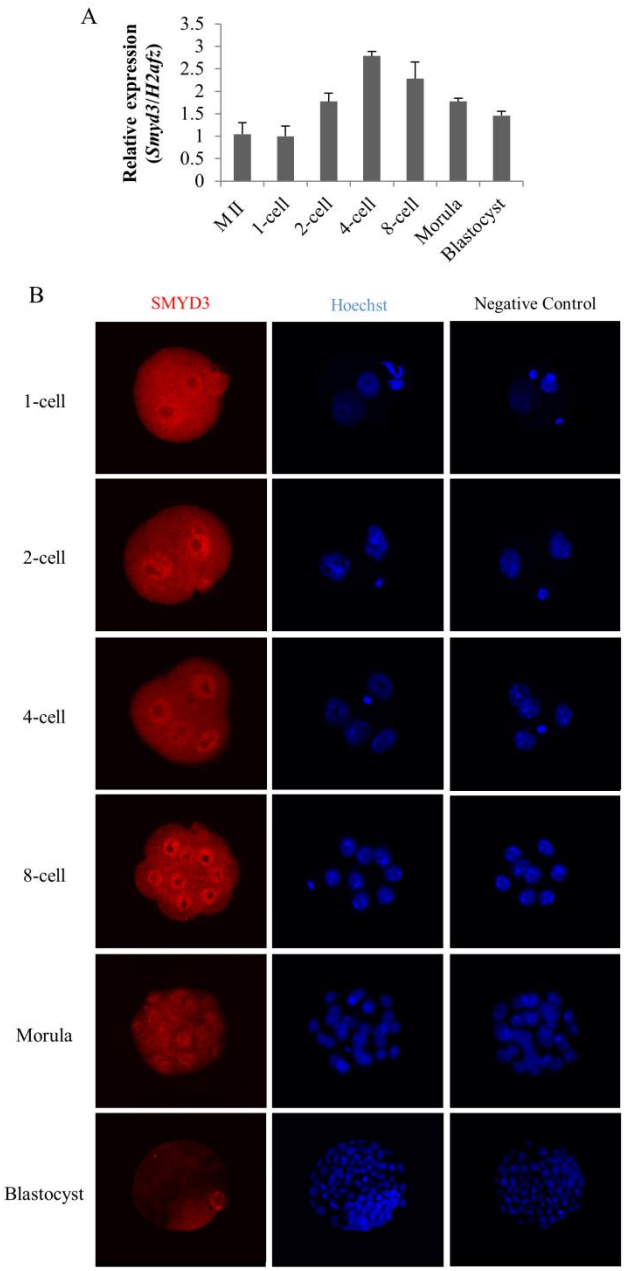

Figure 6. *Smyd3* expression and the localization of SMYD3 in preimplantation embryos.

(A) qRT-PCR analysis of *Smyd3* expression in preimplantation embryos. The expression levels at each developmental stage were normalized by using *H2afz* as an internal control. Data are expressed as mean ± SEM (n=3). (B) Localization of *Smyd3* in mouse preimplantation embryos. SMYD3 (red) is detected by immunofluorescence and nuclei (blue) are stained with Hoechst dye.

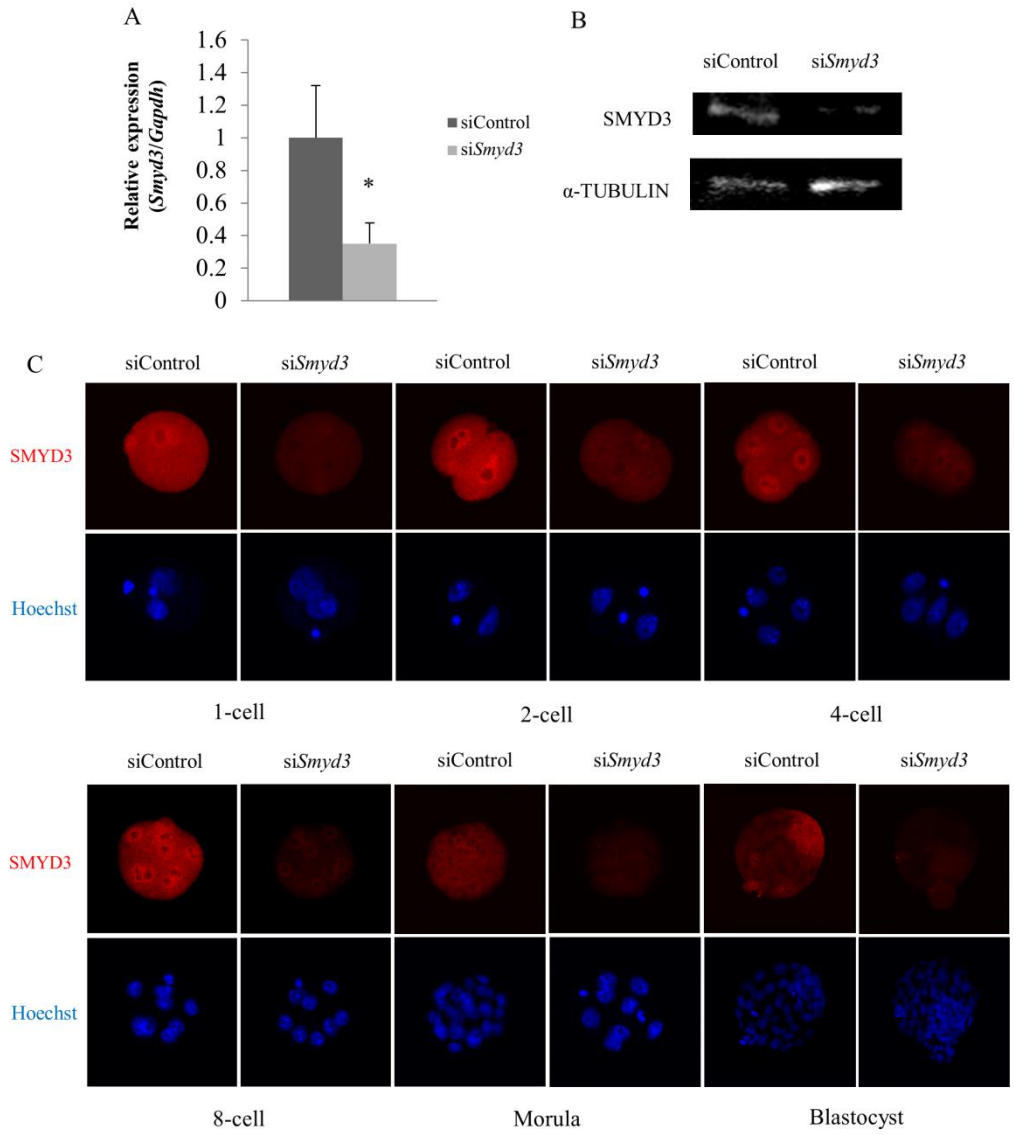

Figure 7. Reduction in the expression of *Smyd3* mRNA and protein at the blastocyst stage.

(A) qRT-PCR analysis of *Smyd3* mRNA at the blastocyst stage in *Smyd3*-knockdown and control embryos (*$p < 0.05$). The expression levels were normalized by using *Gapdh* as an internal control. Data are expressed as mean ± SEM (n=3). (B) Immunoblot analysis of SMYD3 and α-TUBULIN in *Smyd3*-knockdown and control blastocyst embryos. (C) Immunostaining of SMYD3 protein in *Smyd3*-knockdown and control blastocyst embryos (red, SMYD3; blue, chromatin).

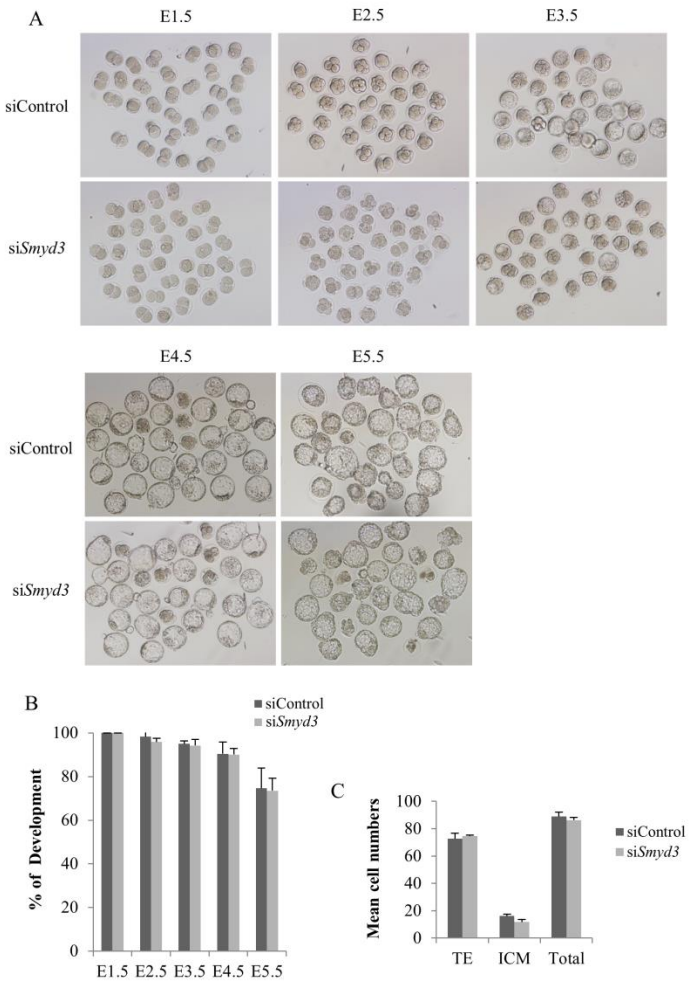

Figure 8. The effects of *Smyd3* knockdown on pre-implantation development.

(A) Pairs of representative photos showing the development of preimplantation embryos injected with either si*Smyd3* or siControl. Embryos were photographed at 36 h after in vitro fertilization and 24 h intervals thereafter. (B) The percentage of development at E1.5 (≥ 2-cell), E2.5 (≥ 4-cell), E3.5 (≥ morula), E4.5 (≥ blastocyst), and E5.5 (≥ hatching) in *Smyd3*-knockdown and control embryos. Data are expressed as mean ± SEM (n=3). Twenty to 25 embryos were used in each experiment (63 and 69 embryos in total in siControl and si*Smyd3*, respectively). (C) The numbers of ICM and TE cells were assessed by counting OCT4-positive cells and CDX2-positive cells, respectively. Total embryonic cell numbers were obtained by combining the numbers of ICM and TE cells. Data are expressed as mean ± SEM (n=16).

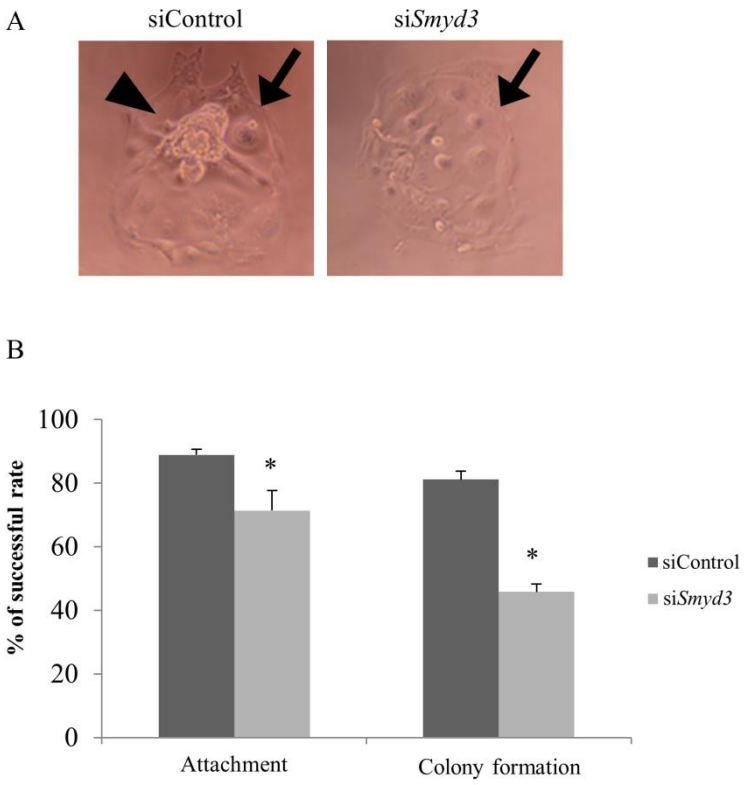

Figure 9. The effects of *Smyd3* knockdown on post-implantation development.

(A) Outgrowth experiments on zona-free embryos were performed. Pictures show representative results (ICM-derived colony, arrowhead; trophectoderm cells, arrow). (B) The successful percentages of attachment and ICM-derived colony formation in *Smyd3*-knockdown and control embryos after 4 days in culture (*$p < 0.05$). Data are expressed as mean ± SEM (n=6). Thirteen to 83 embryos were used in each experiment (238 and 243 embryos in total in siControl and si*Smyd3*, respectively).

Table 6. Effect of *Smyd3*-knockdown on mouse embryo development.

	No. traials (No. recipient mice)	No. embryos transferred	No. pregnant mice	No. live offspring (mean ± SD)	% live offspring
siControl	4	60*	4	31 (7.8±0.25)	51.7
si*Smyd3*	4	60*	4	12 (3.0±0.41)	20.0**

* Fifteen embryos were transferred to each recipient at the trial.

** $p < 0.05$

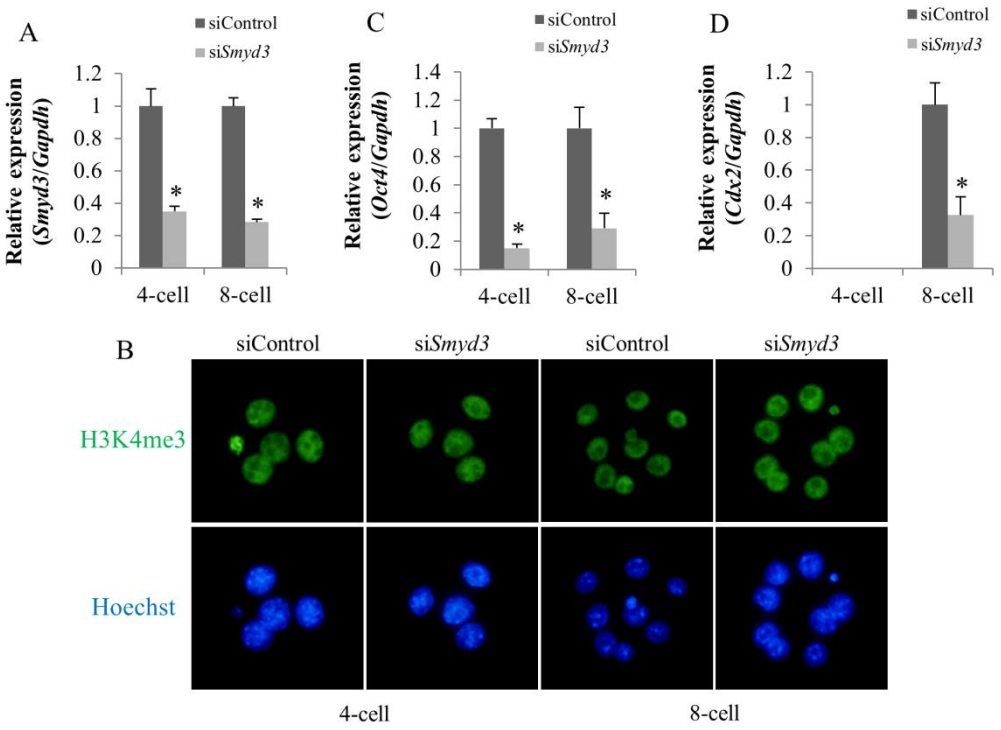

Figure 10. SMYD3 regulates the expression of *Oct4* and *Cdx2* at MGA.

(A) qRT-PCR analysis of *Smyd3* mRNA in *Smyd3*-knockdown and control embryos at the 4- and 8-cell stages (*$p < 0.05$). Expression levels were normalized to *Gapdh* as an internal control. Data are expressed as mean ± SEM (n=3). (B) Immunostaining of H3K4me3 in *Smyd3*-knockdown and control embryos at the 4- and 8-cell stages (red, SMYD3; green, H3K4me3; blue, chromatin). (C and D) qRT-PCR analysis of *Oct4* mRNA and *Cdx2* mRNA in *Smyd3*-knockdown and control embryos at the 4- and 8-cell stages (*$p < 0.05$). Data are expressed as mean ± SEM (n=3).

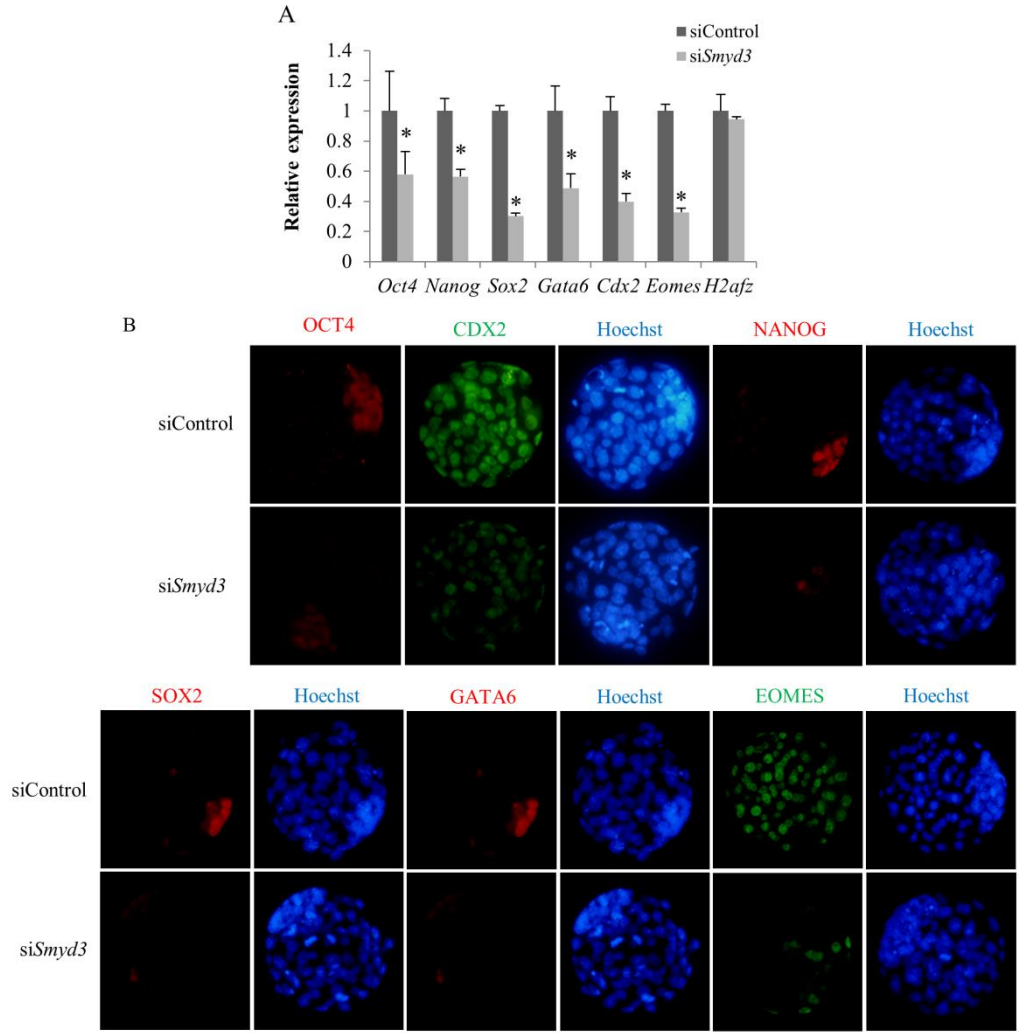

Figure 11. The effects of *Smyd3* knockdown on the expression of lineage-specific genes in blastocysts.

(A) qRT-PCR analysis of the early-lineage markers *Oct4*, *Nanog*, *Sox2*, *Cdx2*, *Eomes*, *Gata6*, and *H2afz* in *Smyd3*-knockdown and control blastocyst embryos (*$p < 0.05$). The expression levels were normalized by using *Gapdh* as an internal control. Data are expressed as mean ± SEM (n=3). (B) Immunostaining of OCT4, CDX2, NANOG, SOX2, GATA6, and EOMES in *Smyd3*-knockdown and control blastocyst embryos (OCT4, red; CDX2, green; NANOG, red; SOX2, red; GATA6, red; EOMES, green; chromatin, blue).

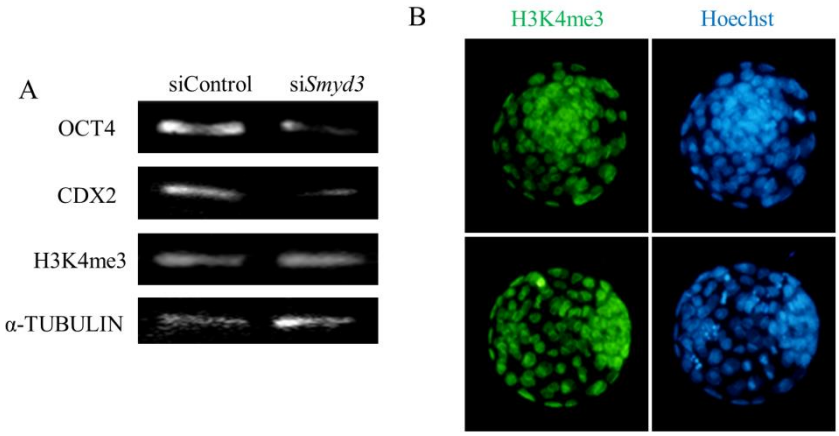

Figure 12. Knockdown of *Smyd3* influence the levels of OCT4 and CDX2 proteins not the levels of H3K4me3.

(A) Immunoblot analysis of OCT4, CDX2, H3K4me3, and α-TUBULIN in *Smyd3*-knockdown and control blastocyst embryos. (B) Immunostaining of H3K4me3 in *Smyd3*-knockdown and control blastocyst embryos (H3K4me3, green; chromatin, blue).

Discussion

SMYD3 methylates both H3K4 and H4K5 (Hamamoto et al; Van Aller et al), recruits RNA polymerase II through an RNA helicase to form a transcription complex, and elicits its oncogenic effects by activating the transcription of downstream target genes (Hamamoto et al; Hamamoto et al; Liu et al; Liu et al). SMYD3 is also involved in apoptosis and the inhibition of cell growth, migration, and invasion (Xu et al, 2006; Zou et al). Here, we observed *Smyd3* mRNA expression patterns and protein localization during mouse preimplantation development, and showed that *Smyd3* knockdown led to a defect in their ability to attach to a matrix and outgrowth *in vitro*, and to a reduction in the numbers of viable offspring, suggesting that SMYD3 has important roles during peri-implantation development.

Previous reports have shown that *Oct4* and *Sox2* form an *Oct4*/*Sox2* complex and bind directly to their own promoter regions in embryonic stem (ES) cells (Chew et al; Okumura-Nakanishi et al). *Oct4*, *Nanog*, and *Sox2* are reported to be regulated via the *Oct4*/*Sox2* complex, and to form a self-reinforcing regulatory loop in ES cells (Chew et al; Mitsui et al; Okumura-Nakanishi et al; Rodda et al). In mouse preimplantation embryos, *Oct4*, *Nanog*, and *Sox2* are required for the maintenance of ICM pluripotency (Avilion et al; Mitsui et al; Nichols et al). Additionally, *Nanog* is known to negatively interact with *Gata6* and both genes are known as key regulators in the establishment of EPI and PE fates, respectively (Frankenberg et al, 2011; Kang et al, 2013; Morris et al, 2010; Schrode et al, 2014). *Nanog* deficient mouse embryos are arrested during post-implantation development due to widespread expression of *Gata6* in the EPI (Frankenberg et al, 2011; Mitsui et al, 2003). By contrast, *Gata6* deficient mouse embryos are arrested during post-implantation development due to widespread expression of *Nanog* in the PE (Morris et al, 2010; Schrode et al, 2014). In this study, we showed that *Smyd3* knockdown led to the suppression of the embryonic transcription of *Oct4*

from the 4-cell stages. Furthermore, we also showed that, in blastocysts, *Smyd3* knockdown abrogates the transcription of other ICM and EPI markers, e.g., *Nanog* and *Sox2*; and of PE markers, such as *Gata6*. Therefore, it is possible that the lack of pluripotency genes, such as *Oct4*, *Nanog*, and *Sox2*; and of PE-specific genes, such as *Gata6*, could account for the defects observed in *Smyd3*-knockdown embryos, including poor outgrowth *in vitro* and a reduction in the numbers of viable offspring. Furthermore, *Cdx2* and *Eomes* are reported to be essential for the specification and differentiation of TE (Russ et al; Strumpf et al). *Cdx2*-knockout embryos fail to hatch from the zona pellucida or to implant *in vivo*, and also fail to attach to matrix substrates *in vitro*, even when the zona pellucida has been removed (Strumpf et al). In this study, we showed that *Smyd3* knockdown led to the suppression of the embryonic transcription of *Cdx2* from the 8-cell stages. Furthermore, we also showed that, in blastocysts, *Smyd3* knockdown abrogates the transcription of TE markers, such as *Eomes*. Therefore, it is possible that the suppression of TE-specific genes, such as *Cdx2* and *Eomes*, could account for a defect in their ability to attach to a matrix substrate *in vitro* observed in *Smyd3*-knockdown embryos. Together, these observations also suggested that SMYD3 plays an important role in peri-implantation embryonic development. However, we demonstrated that in *Smyd3*-knockdown embryos global H3K4me3 levels appeared unchanged and that developmental arrest did not occur up to the blastocyst stage, even though *Smyd3* knockdown suppressed that SMYD3 proteins dominantly localized in the nuclei at ZGA and MGA. Previous studies showed that MLL2, one of the H3K4 methyltransferases, affected the global H3K4me3 levels at ZGA (Andreu-Vieyra et al), and the SETD1A/SETD1B methyltransferase complex that modifies H3K4 affected the global H3K4me3 levels at MGA (Bi et al). Additionally, previous studies demonstrated that a knockdown of SMYD3 expression led to the selective decrease in H3K4 methylation levels on oncogene promoter regions in cancer cells (Cock-Rada et al; Liu et

al; Medjkane et al). From these observations it is possible that H3K4me3 level depends on the type of methyltransferase and that SMYD3 modified H3K4 within the promoter regions of the lineage-specific genes. In addition, a recent report demonstrated that while global levels of H3K4me3 do not change upon the loss of *Smyd3* in the human breast carcinoma cell line, MCF7, the global levels of H4K5me, a novel chromatin target of *Smyd3*, do change (Van Aller et al). This result indicates that SMYD3 is required for H4K5 methylation in cancer cells. It is also possible that SMYD3 is involved in the regulation of genes in mouse preimplantation embryos through the methylation of H4K5.

In summary, our results demonstrated that *Smyd3*-knockdown does not have a critical effect on early embryonic development or on global H3K4me3 levels, but that it does play an important role in early embryonic lineage commitment and peri-implantation development by regulating the expression of *Oct4* and *Cdx2* at MGA. Accordingly, we demonstrated the importance of *Smyd3* as a key regulator of lineage-specific genes in mouse preimplantation embryos.

Chapter 4

CHD1 acts via the *Hmgpi* pathway to regulate cell fate specification during mouse preimplantation development

Abstract

CHD1 is a protein belonging to the family of ATPase-dependent chromatin remodeling factors. CHD1 recognizes trimethylated histone H3 lysine 4, has been implicated in transcriptional activation from yeast to humans, and is required for pre-mRNA maturation and maintenance of mouse ES cell pluripotency. However, the function(s) of CHD1 in mouse preimplantation embryos has not yet been examined. Here, we show that loss of CHD1 function led to embryonic lethality after implantation. In embryos where *Chd1* was targeted by siRNA microinjection, the expression of *Oct4* (also known as *Pou5f1*) and *Cdx2*—key regulators of cell fate specification—was dramatically decreased from mid-preimplantation gene activation (MGA). Moreover, expression of *Hmgpi* and *Klf5*, which regulate *Oct4* and *Cdx2*, was also significantly decreased at zygotic gene activation (ZGA). Suppression of *Hmgpi* expression in *Chd1*-knockdown embryos continued until the blastocyst stage, while the suppression of *Klf5* expression was relieved by the morula stage. Next, we rescued HMGPI expression via *Hmgpi* mRNA microinjection in *Chd1*-knockdown embryos. Consequently, *Oct4* and *Cdx2* expression was restored at MGA and live offspring were recovered. These findings indicated that CHD1 plays important roles in cell fate specification and the development of mouse postimplantation embryos via the activation of *Hmgpi* at ZGA. This is the first report that demonstrates the relevance of ZGA and cell-fate specification in mouse embryogenesis.

Introduction

During preimplantation development in the mouse, the first important gene expression event is zygotic gene activation (ZGA), the first transcription from the newly formed zygotic genome, which occurs between the late 1-cell and 2-cell stages and is required for normal development (Hamatani et al, 2004; Levey et al, 1977; Li et al, 2010; Minami et al, 2007; Schultz, 1993; Wang & Dey, 2006; Warner & Versteegh, 1974). One-cell embryos treated with α-amanitin, an RNA polymerase II inhibitor, arrest development at the 2-cell stage because ZGA is suppressed (Levey et al, 1977; Warner & Versteegh, 1974). The second transcriptional event is mid-preimplantation gene activation (MGA), which occurs between the 4-cell and 8-cell stages. During this period, genes required for cell fate specification, e.g., the transcription factors *Oct4* (*Pou5f1*) and *Cdx2*, are expressed; these genes are known to be key regulators governing differentiation of the inner cell mass (ICM) and trophectoderm (TE) (Hamatani et al, 2004; Nichols et al, 1998; Niwa et al, 2005; Strumpf et al, 2005; Wang & Dey, 2006; Yoshikawa et al, 2006). Thus, to understand cell fate specification, we must discern the regulatory mechanisms of *Oct4* and/or *Cdx2* expression at MGA. A previous study showed that a deficiency of *Tead4*, a transcription factor expressed during ZGA in mouse preimplantation embryos, led to a failure of cell fate specification due to the suppression of *Cdx2* expression at MGA and developmental arrest at the morula stage (Yagi et al, 2007). Other experiments have also identified genes that are involved in cell fate specification through regulating the expression of *Oct4* and/or *Cdx2* (Do et al, 2013; Elling et al, 2006; Home et al, 2012; Strumpf et al, 2005; Wang et al, 2010; Zhang et al, 2006; Zhang et al, 2013), gradually clarifying the regulatory mechanisms underlying *Oct4* and/or *Cdx2* expression.

Dynamic changes occur in chromatin structure during preimplantation development in mammals (Abdalla et al, 2009; Albert & Helin, 2010; Burton & Torres-Padilla, 2010; Corry et al,

2009; Morgan et al, 2005; Rasmussen & Corry, 2010; Shi & Wu, 2009). Previous studies showed that suppression of *Brg1*, a subclass of SWItch/Sucrose Non-Fermentable (SWI/SNF) ATP-dependent chromatin remodelers, in mouse preimplantation embryos causes the widespread expression of *Oct4* in the TE and leads to early embryonic death (Kidder et al, 2009; Wang et al, 2010). This result suggests that chromatin-remodeling factors play important roles in mouse cell fate specification. CHD1 (chromodomain helicase DNA binding protein 1) is a protein belonging to the family of ATPase-dependent chromatin remodeling factors (Woodage et al, 1997). CHD1 recognizes the trimethylated lysine 4 of histone 3 (H3K4me3) (Sims et al, 2005) and has been implicated in transcriptional activation in yeast (Simic et al, 2003), *Drosophila* (Stokes et al, 1996), and mammalian cells (Sims et al, 2007). CHD1 is involved in pre-mRNA maturation (Sims et al, 2007), the maintenance of mouse ES cell pluripotency (Gaspar-Maia et al, 2009), and incorporation of the variant histone H3.3 into paternal pronuclear chromatin at fertilization in *Drosophila* embryos (Konev et al, 2007). However, the function(s) of CHD1 in mammalian preimplantation development is unknown.

In the present study, we investigated whether CHD1 functions during preimplantation development in the mouse. We observed that *Chd1* expression started to increase at the 2-cell stage, CHD1 was intensely localized in the nuclei from the 2-cell stage, and loss of CHD1 function by siRNA treatment led to embryonic lethality after implantation due to the suppression of *Oct4* and *Cdx2* expression at MGA. Additionally, the expression of *Hmgpi* and *Klf5*, which regulate the expression of *Oct4* and *Cdx2* during mouse preimplantation development (Ema et al, 2008; Lin et al, 2010; Yamada et al, 2010), was dramatically decreased beginning at ZGA. However, *Hmgpi* mRNA microinjection in *Chd1*-knockdown embryos (*Chd1*-knockdown-*Hmgpi*-rescue embryos) rescued *Oct4* and *Cdx2* expression and postimplantation embryo development. Based on these results, we propose that CHD1 has

important roles in the development of pre- and postimplantation embryos via the activation of *Hmgpi* expression at ZGA.

Materials and Methods

Superovulation, embryo collection, and embryo culture

Eight- to 10-week-old ICR female mice (Japan SLC, Hamamatsu, Japan) were superovulated by injecting 5 IU of equine chorionic gonadotropin (eCG; ASUKA Pharmaceutical Co., Ltd., Tokyo, Japan) followed by 5 IU of human chorionic gonadotropin (hCG; ASUKA Pharmaceutical Co., Ltd.) 48 h later. Unfertilized eggs were harvested 14 h after the hCG injection and placed in a 90-μL droplet of mHTF supplemented with 4 mg/mL BSA (A3311; Sigma-Aldrich, St. Louis, MO) (Minami et al, 2001). Spermatozoa were collected from the cauda epididymis of 11- to 15-week-old ICR male mice (Japan SLC) and cultured for 2 h in 100-μL of HTF supplemented with 4 mg/mL BSA. After preincubation, sperm were introduced into fertilization droplets at a final concentration of 1×10^6 cells/mL. After a 3-h incubation, fertilized 1-cell embryos were collected and washed 3 times in KSOM supplemented with amino acids (Ho et al, 1995) and 4 mg/mL BSA, and then were either used for microinjection or cultured until embryonic day 4.5 (E4.5) in the same medium under mineral oil (Sigma-Aldrich) at 37 °C in an atmosphere of 5% CO_2.

Chd1 siRNA injection

Approximately 5–10 pL of 100 μM *Chd1* siRNA (si*Chd1*) (RNAi Inc., Japan, 5'-GGUUUACUUAGGCGACAUUAA-3') or the control scrambled sequence siRNA (siControl; RNAi Inc.) (5'-GCGUUUAUAGCAUAUUGCGAA-3') in annealing buffer consisting of 30 mM HEPES-KOH (pH 7.4), 100 mM KOAc, and 2 mM $Mg(OAc)_2$ was microinjected into the cytoplasm of 1-cell embryos between 3 and 4 h after insemination. After injection, the embryos were cultured in KSOM medium supplemented with amino acids (Ho et al, 1995) with 4 mg/mL BSA under mineral oil (Sigma-Aldrich) at 37 °C in an atmosphere of 5% CO_2. To examine developmental competency and hatching ability, embryos were observed

at 36 (E1.5), 60 (E2.5), 84 (E3.5), 108 (E4.5), and 132 h (E5.5) after insemination. Furthermore, the embryos were harvested for quantitative RT-PCR (qRT-PCR), immunofluorescent staining, outgrowth analysis, or embryo transfer.

RNA extraction and qRT-PCR

Embryos were harvested after culturing for 14, 20, 36, 48, 55, 76, and 108 h after insemination, when the most of the oocytes reached the 1-cell, early 2-cell, late 2-cell, 4-cell, 8-cell, morula, and blastocyst stages, respectively. RNA extraction and qRT-PCR were performed as described previously (Suzuki et al, 2013). Total RNA from 30 embryos was extracted using the TRIzol reagent (Invitrogen, Carlsbad, CA). Transcription levels were determined on three different sets of 30 embryos per stage and normalized to *Gapdh*; relative gene expression was analyzed using the $2^{-\Delta\Delta Ct}$ method (Livak & Schmittgen, 2001). The primers used for qPCR are listed in Table 7.

Immunofluorescent staining

Embryos for immunostaining were collected as described above. For staining of CHD1, HMGPI, and KLF 5, zona pellucida was removed from the embryo by acid Tyrode's solution (pH 2.5) (Table 7) and the embryos were fixed in phosphate buffered saline (PBS) containing 4% paraformaldehyde (Sigma-Aldrich) for 20 min at 4 °C. After washing three times in PBS containing 0.3% polyvinylpirrolidone (PVP K-30, Nacalai Tesque, Kyoto, Japan; PBS/PVP), embryos were treated with 0.5% Triton X-100 (Sigma-Aldrich) in PBS for 40 min at room temperature (RT), blocked in PBS containing 1.0% BSA (A9647, Sigma-Aldrich) for 1 h at RT (for CHD1 and KLF5) or 3.0% BSA overnight at 4 °C (for HMGPI), and then incubated overnight at 4 °C with a rabbit anti-CHD1 antibody (1:25 dilution, #4351, Cell Signaling Technology, Inc., Beverly, MA) or a rat anti-KLF5 antibody (1:500 dilution) (Shindo et al, 2002) or for 1 h at RT with a rabbit anti-HMGPI antibody (1:100 dilution) (Yamada et al, 2010)

in PBS containing 1.0% BSA (PBS/BSA). After washing with PBS/BSA, embryos were incubated in PBS/BSA containing a secondary antibody (Alexa Fluor 594 goat anti-rabbit IgG, 1:250 dilution, Invitrogen; Alexa Fluor 488 goat anti-rat IgG, 1:300 dilution, Invitrogen; or Alexa Fluor 488 goat anti-rabbit IgG, 1:500 dilution, Invitrogen) for 1 h at RT. After washing three times in PBS/BSA for 15 min each, nuclei were stained in PBS/BSA containing 10 μg/mL Hoechst 33342 (Sigma-Aldrich) for 10 min. Immunostaining with normal rabbit IgG (sc-2027, Santa Cruz Biotechnology Inc., Dallas, TX) was included as a negative control for the specificity of the anti-CHD1 antibody. For staining of OCT4 and CDX2, immunofluorescent staining was performed as previously described (Isaji et al, 2013). After immunofluorescent staining, embryos were mounted on slides in 50% glycerol/PBS and fluorescent signals were detected with a fluorescence microscope (BX50, Olympus, Tokyo, Japan). At least 30 oocytes were examined in each group.

Outgrowth analysis

Outgrowth analysis was carried out on E3.5 embryos after removal of the zona pellucida by acid Tyrode's solution (pH 2.5). The embryos were cultured in ES medium (Glasgow modification of Eagle's medium; GMEM; Invitrogen) supplemented with 10% fetal bovine serum (FBS), 1 mM sodium pyruvate (Sigma), 0.1 mM MEM nonessential amino acid (Invitrogen), 0.1 mM 2-mercaptoethanol (Wako Pure Chemical Industries, Ltd., Osaka, Japan), 0.1 mM L-glutamine, 100 units/mL penicillin, and 100 μg/mL streptomycin (Invitrogen) on a 0.1% gelatin-coated dish (Sigma-Aldrich) at 37 °C in an atmosphere of 5% CO_2. After 4 days in culture, the embryos were photographed and the percentage of blastocysts that had undergone outgrowth was calculated.

Embryo transfer

Two-cell embryos developed after microinjection were transferred into the oviducts of

surrogate females (Japan SLC) that were mated with vasectomized males the day before embryo transfer. These females were sacrificed at day 19 and pups were counted.

In vitro transcription and microinjection

The *Hmgpi* ORF was generated by PCR from mouse embryonic stem cell cDNA. For construction of an *Hmgpi* expression vector, the *Hmgpi* ORF was digested by AgeI and BamHI, and the fragment was cloned into the pAcGFP1-C1 vector plasmid (Clontech Laboratories, Mountain View, CA). The plasmid, digested by MluI, was used as template for in vitro transcription. RNA synthesis and poly(A) tailing were performed with a MEGAscript T7 kit (Invitrogen). Approximately 5–10 pL of 100 ng/μL *Hmgpi* mRNA in DEPC water (Invitrogen) was microinjected into the embryonic cytoplasm just after microinjection of si*Chd1*. The primers used for cloning are listed in Table 8.

Statistical Analysis

Each experiment was repeated at least three times. All data are expressed as the mean ± SEM. Statistical analysis of the data was performed by analysis of variance (ANOVA) with the Student's *t*-test. p values < 0.05 were considered to be statistically significant.

Ethical approval for the use of animals

All animal experiments were approved by the Animal Research Committee of Kyoto University (Permit Number: 24-17) and performed in accordance with the guidelines of the committee.

Table 7. Primers used for qRT-PCR

Genes	GeneBank Accession No.	Forward	Reverse
Chd1	NM_007690.3	aagtcgacggagccgagt	cattgcagatctctggacagc
Oct4	NM_001252452.1	atggggaaagaagctcagtg	caaaatgatgagtgacagacagg
Cdx2	NM_007673.3	agctgctgtaggcggaatgtatg	tcagtgactcgaacagcagcaa
Hmgpi	NM_001033793.3	gttgggagttggactatggac	tgaactgattggacacacaca
Klf5	NM_009769.4	agcctggaagtcccgataga	attgtagcggcataggacgg
Gapdh	NM_001289726.1	cgtgttcctacccccaatgt	tgtcatcatacttggcaggtttc

Table 8. Primers used for *Hmgpi* cloning

Hmgpi Forward	gggaccggttaatacgactcactatagggtttgcactaatgacatcac
Hmgpi Reverse	gggggatccttaatcatcttcatctgtac

Results

Expression and localization of *Chd1* during preimplantation development in the mouse

To investigate the roles of CHD1 during preimplantation development in the mouse, *Chd1* expression and CHD1 localization were examined in preimplantation embryos. *Chd1* mRNA was expressed from the 1-cell to the blastocyst stage. Specifically, the expression increased at the 2-cell stage, peaked at the 8-cell stage, and then dramatically decreased (Fig. 13A). CHD1 was localized in the nuclei of all blastomeres during preimplantation development and its staining intensity increased from the 2-cell stage onward (Fig. 13B).

Loss of CHD1 function causes the loss of ICM pluripotency

Although the results of qRT-PCR and immunostaining showed that the amounts of *Chd1* mRNA and protein were dramatically decreased after the 2-cell stage when si*Chd1* was injected at the 1-cell stage (Fig. 14, A and B), abnormal embryo development was not observed until the blastocyst stage and there were no differences in hatching percentages between control and *Chd1*-knockdown embryos (Fig. 15, A and B). However, outgrowth experiments showed that the percentage of ICM-derived colony formation was dramatically decreased in *Chd1*-knockdown embryos (Fig. 15, C and D). Furthermore, the litter size after embryo transfer was significantly reduced in *Chd1*-knockdown embryos (Table 9).

CHD1 regulates zygotic expression of *Oct4* and *Cdx2*

To investigate the cause of litter size reduction in *Chd1*-knockdown embryos, expression of the early differentiation markers, Oct4 and Cdx2, was assessed at the mRNA and protein levels by qRT-PCR and immunostaining, respectively. With respect to *Oct4* (Fig. 16A), in control embryos mRNA levels were dramatically increased at the 4- and 8-cell stages, and then decreased. By contrast, *Oct4* mRNA expression was suppressed throughout these stages in *Chd1*-knockdown embryos. With respect to *Cdx2* (Fig. 16B), in control embryos mRNA was

first detected at the 8-cell stage, and then gradually increased. Interestingly, *Cdx2* mRNA expression was suppressed during these stages in *Chd1*-knockdown embryos. Furthermore, in *Chd1*-knockdown embryos immunofluorescent detection of OCT4 and CDX2 revealed that maternal OCT4 protein was maintained until the 4-cell stage, and that newly synthesized OCT4 and CDX2 proteins were reduced from the 8-cell and morula stages, respectively. The localization of OCT4 in the ICM and of CDX2 in the TE did not change in *Chd1*-knockdown embryos (Fig. 16C).

CHD1 regulates the expression of *Hmgpi* and *Klf5* during preimplantation development

It has been reported that knockdown of *Hmgpi* or knockout of *Klf5* during preimplantation development leads to early embryonic lethality due to a reduction in both *Oct4* and *Cdx2* expression (Ema et al, 2008; Lin et al, 2010; Yamada et al, 2010). To investigate the effects of CHD1 on *Hmgpi* and *Klf5* expression, the levels of *Hmgpi* and *Klf5* mRNA and protein in *Chd1*-knockdown embryos were examined by qRT-PCR and immunostaining. With respect to *Hmgpi* (Fig. 17A), in control embryos mRNA was first detected at the late 2-cell stage, peaked at the 4-cell stage, and then gradually decreased. Conversely, *Hmgpi* mRNA expression was suppressed during these stages in *Chd1*-knockdown embryos. Immunofluorescent detection of HMGPI determined that HMGPI protein levels were also reduced from the 4-cell stage onward in *Chd1*-knockdown embryos (Fig. 17B). With respect to *Klf5* (Fig. 17C), in control embryos mRNA was also first detected at the late 2-cell stage, peaked at the 8-cell stage, and was maintained through the blastocyst stage. On the other hand, in *Chd1*-knockdown embryos, expression was suppressed at the 4- and 8-cell stages but recovered after the morula stage. Immunofluorescent detection of KLF5 demonstrated that the amount of KLF5 protein was remarkably reduced at the 4- and 8-cell stages; however, KLF5 protein levels gradually recovered after the morula stage in *Chd1*-knockdown embryos (Fig.

17D).

HMGPI rescue can recover outgrowth and litter size in *Chd1*-knockdown embryos

To investigate whether *Hmgpi* regulates the expression of *Oct4* and *Cdx2* under the control of CHD1, HMGPI expression was rescued by the injection of *Hmgpi* mRNA in *Chd1*-knockdown embryos. Outgrowth and embryo transfer experiments showed that normal ICM-derived colony formation and litter size were recovered in *Chd1*-knockdown-*Hmgpi*-rescue embryos (Fig. 18, A and B, Table 10). qRT-PCR results indicated that *Chd1* mRNA levels were not restored in *Chd1*-knockdown-*Hmgpi*-rescue embryos at any stage (Fig. 18C). Nonetheless, qRT-PCR and immunostaining results showed that *Oct4* mRNA levels were recovered from the 4-cell stage onward, and that OCT4 protein expression was recovered from the 8-cell stage onward (because maternal OCT4 protein remains until the 4-cell stage in *Chd1*-knockdown-*Hmgpi*-rescue embryos). Furthermore, *Cdx2* mRNA levels were restored from the 8-cell stage onward, and CDX2 protein levels were recovered from the morula stage onward in *Chd1*-knockdown-*Hmgpi*-rescue embryos (Fig. 18D-E). Meanwhile, qRT-PCR and immunostaining of *Klf5* showed that HMGPI rescue had no effect on the expression of *Klf5* mRNA or protein (Fig. 19, A and B).

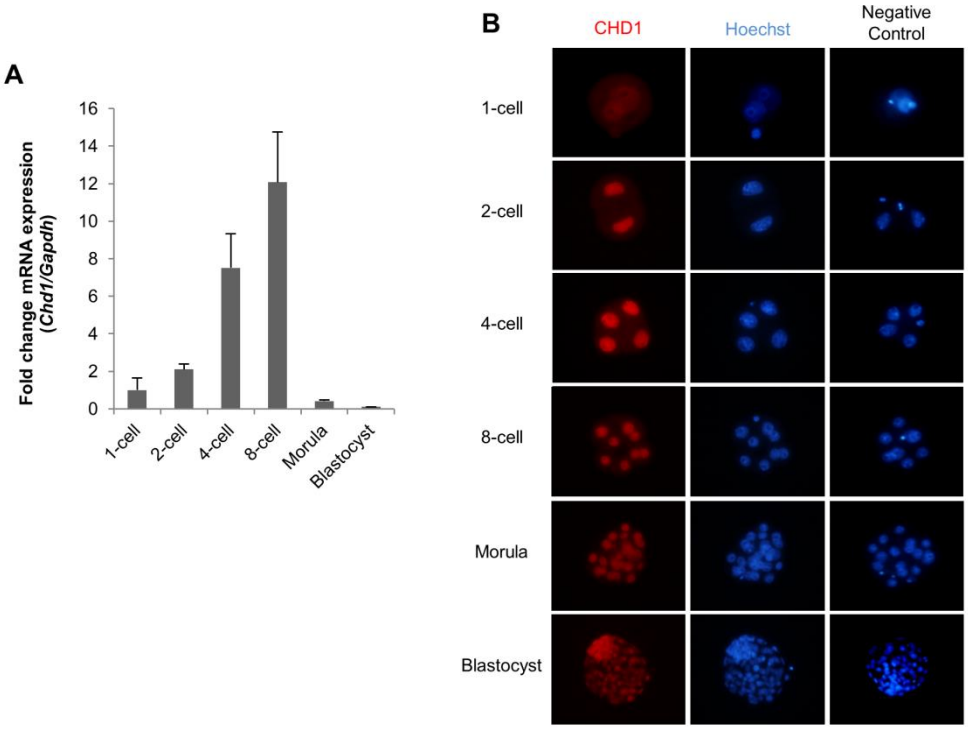

Figure 13. *Chd1* expression and CHD1 localization during mouse preimplantation development.

(A) qRT-PCR analysis of *Chd1* mRNA expression during mouse preimplantation development. The expression levels at each developmental stage were normalized by using *Gapdh* as an internal control. The mRNA levels of the 1-cell embryos were set to 1. Data are expressed as the mean ± SEM (n = 3). (B) Localization of CHD1 during mouse preimplantation development (red, CHD1; blue, chromatin).

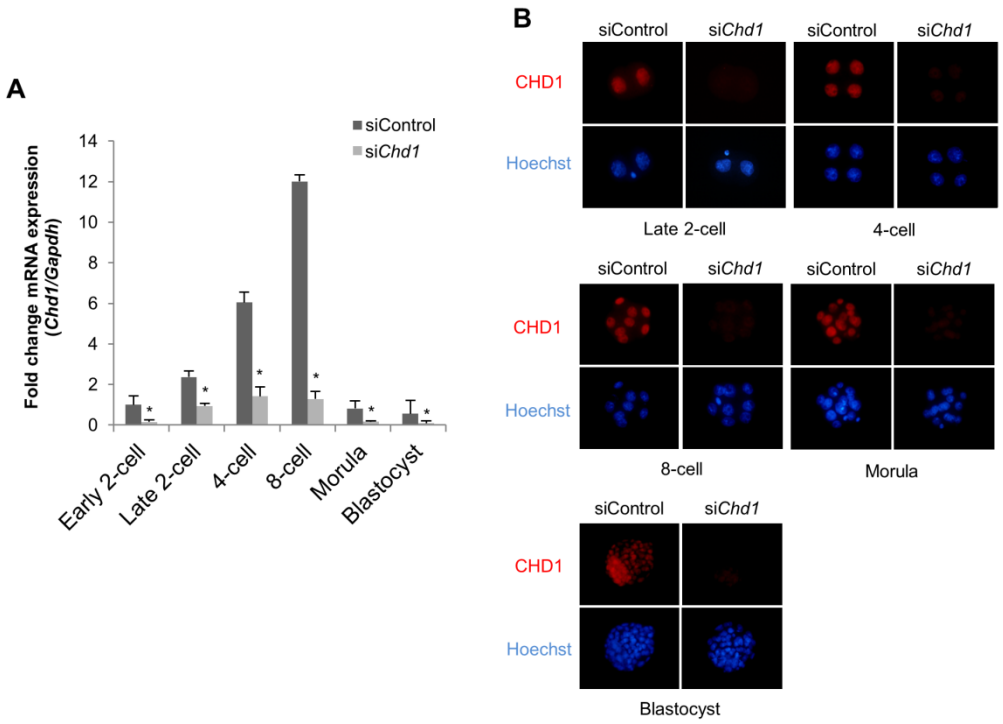

Figure 14. The effects of si*Chd1* injection on the expression of *Chd1* mRNA and protein in mouse preimplantation embryos.

(A) qRT-PCR analysis of *Chd1* mRNA expression in control and *Chd1*-knockdown embryos from the early 2-cell to the blastocyst stages (*$p < 0.05$). Expression levels were normalized to *Gapdh* as an internal control. The mRNA levels of the early 2-cell control embryos were set to 1. Data are expressed as the mean ± SEM (n = 3). (B) Immunofluorescent detection of CHD1 protein in control and *Chd1*-knockdown embryos (red, CHD1; blue, chromatin).

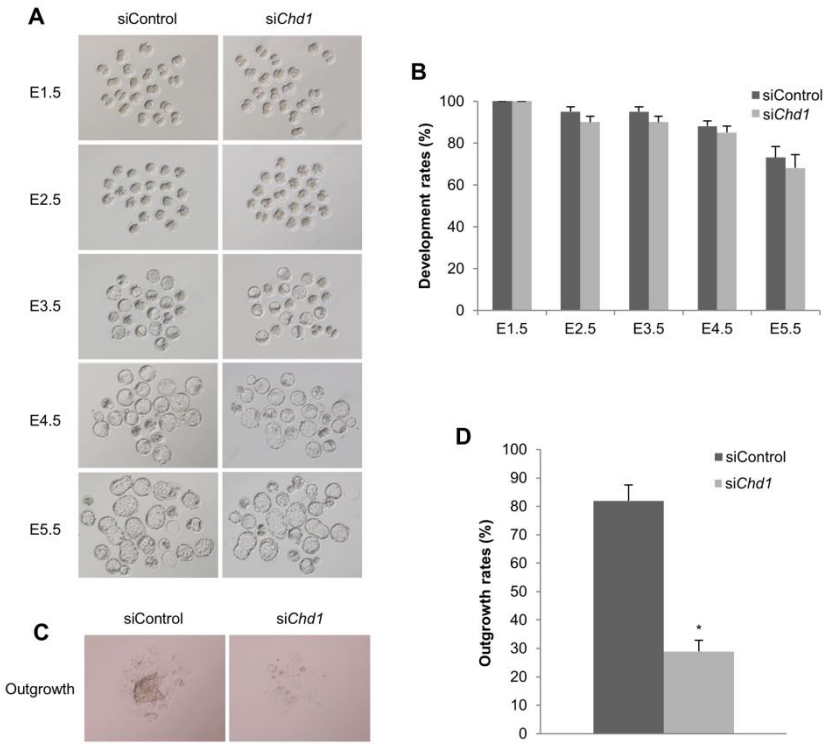

Figure 15. Loss of CHD1 function induces developmental arrest during postimplantation development.

(A) Pairs of representative photos showing the development of preimplantation embryos injected with either siControl or si*Chd1*. Embryos were photographed 36 h after in vitro fertilization and at 24-h intervals thereafter. (B) The percentages of normal development observed at E1.5 (≥ 2-cell), E2.5 (≥ 4-cell), E3.5 (≥ morula), E4.5 (≥ blastocyst), and E5.5 (≥ hatching) in control and *Chd1*-knockdown embryos. Data are expressed as the mean ± SEM (n = 5). Twenty embryos were used in each experiment: 100 embryos each for the siControl and si*Chd1* arms. (C) Photographs depict representative results of outgrowth experiments for control and *Chd1*-knockdown embryos. (D) The successful percentage of ICM-derived colony formation in control and *Chd1*-knockdown embryos after 4 days in culture (*$p < 0.05$). Data are expressed as the mean ± SEM (n = 5). Twenty-five to 120 embryos were used in each experiment: 284 and 218 embryos each for the siControl and si*Chd1* arms.

Table 9. Effect of *Chd1*-knockdown on the development of mouse embryos.

Treatment	No. embryos transferred (No. recipients)	No. live offspring (%)
siControl	45 (3)	22 (48.9)
si*Chd1*	45 (3)	6 (13.3)*

*$p < 0.05$

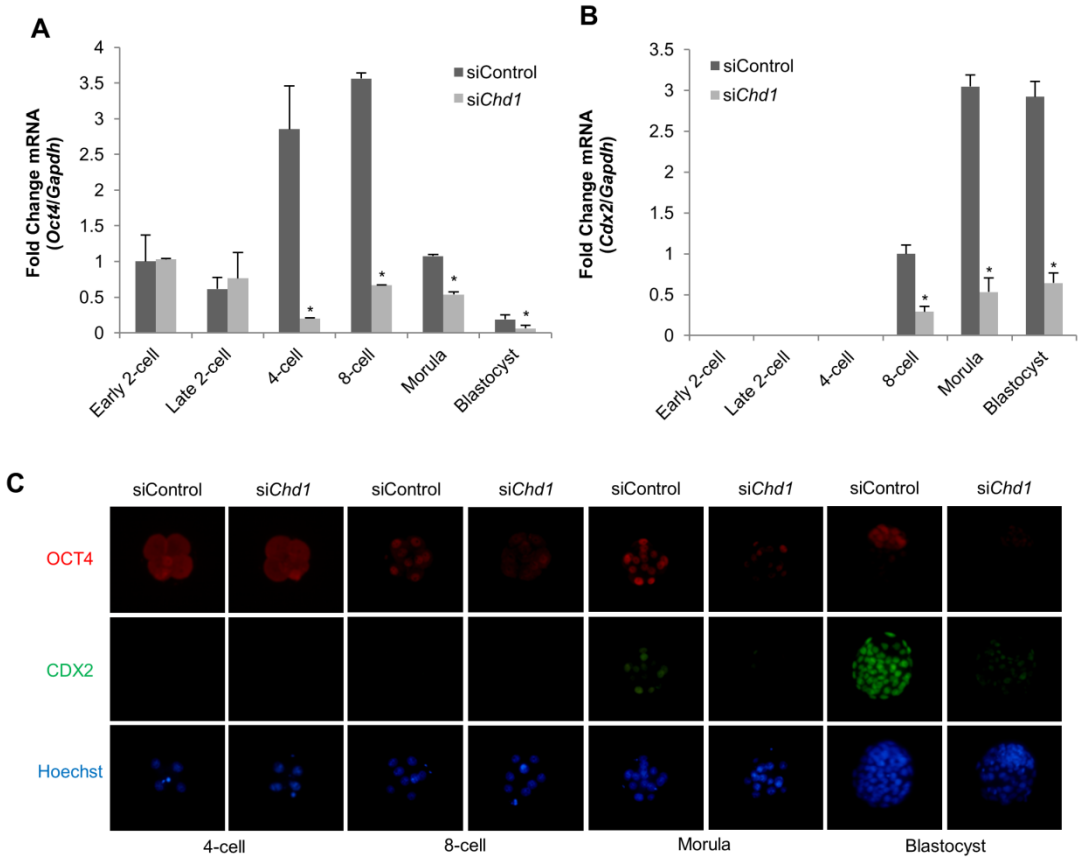

Figure 16. CHD1 is required for cell fate specification.

(A) qRT-PCR analysis of *Oct4* mRNA in control and *Chd1*-knockdown embryos from the early 2-cell to the blastocyst stages (*$p < 0.05$). Expression levels were normalized to *Gapdh* as an internal control. mRNA levels of the early 2-cell control embryos were set to 1. Data are expressed as the mean ± SEM (n = 3). (B) qRT-PCR analysis of *Cdx2* mRNA in control and *Chd1*-knockdown embryos from the early 2-cell to the blastocyst stages (*$p < 0.05$). Expression levels were normalized to *Gapdh* as an internal control. mRNA levels of the 8-cell control embryos were set to 1. Data are expressed as the mean ± SEM (n = 3). (C) Immunofluorescent detection of OCT4 and CDX2 in control and *Chd1*-knockdown embryos (red, OCT4; green, CDX2; blue, chromatin).

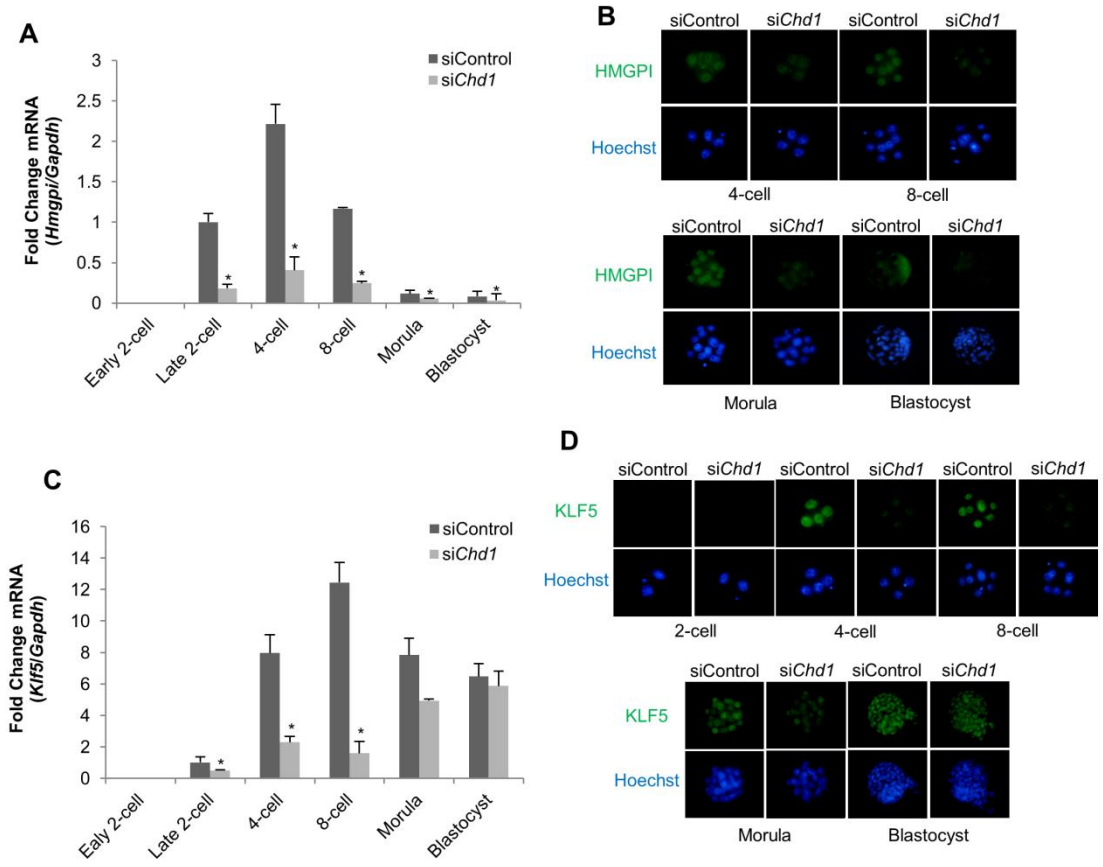

Figure 17. The effects of si*Chd1* injection on *Hmgpi* and *Klf5* expression.

(A) qRT-PCR analyses of *Hmgpi* mRNA in control and *Chd1*-knockdown embryos from the early 2-cell to the blastocyst stages (*$p < 0.05$). The expression levels were normalized to *Gapdh* as an internal control. The mRNA levels of the late 2-cell control embryos were set to 1. Data are expressed as the mean ± SEM (n = 3). (B) Immunofluorescent detection of HMGPI in control and *Chd1*-knockdown embryos (green, HMGPI; blue, chromatin). (C) qRT-PCR of *Klf5* mRNA in control and *Chd1*-knockdown embryos from the early 2-cell to the blastocyst stages (*$p < 0.05$). The expression levels were normalized to *Gapdh*. The mRNA levels of the late 2-cell control embryos were set to 1. Data are expressed as the mean ± SEM (n = 3). (D) Immunofluorescent detection of KLF5 in control and *Chd1*-knockdown embryos (green, KLF5; blue, chromatin).

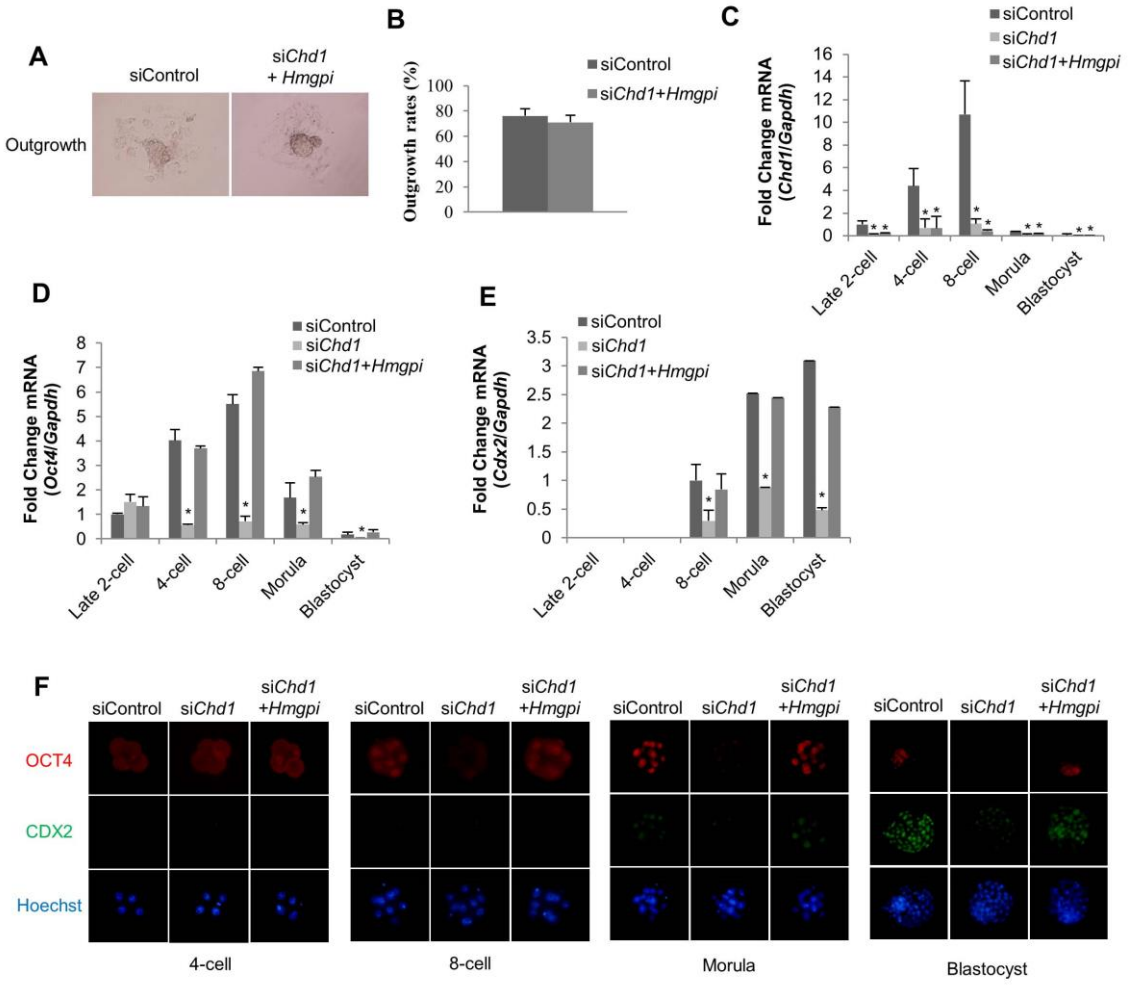

Figure 18. The effects of *Hmgpi*-rescue in *Chd1*-knockdown embryos on cell fate specification and the development of postimplantation embryos.

(A) Photographs depict representative results of outgrowth experiments from control and *Chd1*-knockdown-*Hmgpi*-rescue embryos. (B) The percentage of ICM-derived colony formation in control or *Chd1*-knockdown-*Hmgpi*-rescue embryos after 4 days in culture (*$p < 0.05$). Data are expressed as the mean ± SEM (n = 3). Twenty to 80 embryos were used in each experiment: 172 and 129 embryos total for siControl and si*Chd1*+ *Hmgpi* mRNA, respectively. (C) qRT-PCR analysis of *Chd1* mRNA in control, *Chd1*-knockdown, and *Chd1*-knockdown-*Hmgpi*-rescue embryos from the late 2-cell to the blastocyst stages.

Expression levels were normalized to *Gapdh* as an internal control. The mRNA levels of the late 2-cell control embryos were set to 1. Data are expressed as the mean ± SEM (n = 3). (D) qRT-PCR analysis of *Oct4* mRNA in control, *Chd1*-knockdown, and *Chd1*-knockdown-*Hmgpi*-rescue embryos from the late 2-cell to the blastocyst stages (*$p < 0.05$). Expression levels were normalized to *Gapdh*. The mRNA levels of the late 2-cell control embryos were set to 1. Data are expressed as the mean ± SEM (n = 3). (E) qRT-PCR analysis of *Cdx2* mRNA in control, *Chd1*-knockdown, and *Chd1*-knockdown-*Hmgpi*-rescue embryos from the late 2-cell to the blastocyst stages (*$p < 0.05$). Expression levels were normalized to *Gapdh*. The mRNA levels of the 8-cell control embryos were set to 1. Data are expressed as the mean ± SEM (n = 3). (F) Immunofluorescent detection of OCT4 and CDX2 in control, *Chd1*-knockdown, and *Chd1*-knockdown-*Hmgpi*-rescue embryos (red, OCT4; green, CDX2; blue, chromatin).

Table 10. Effect of *Hmgpi*-rescue on the development of *Chd1*-knockdown embryos.

Treatment	No. embryos transferred (No. recipients)	No. live offspring (%)
siControl	45 (3)	20 (44.4)
si*Chd1* + *Hmgpi mRNA*	45 (3)	22 (48.9)

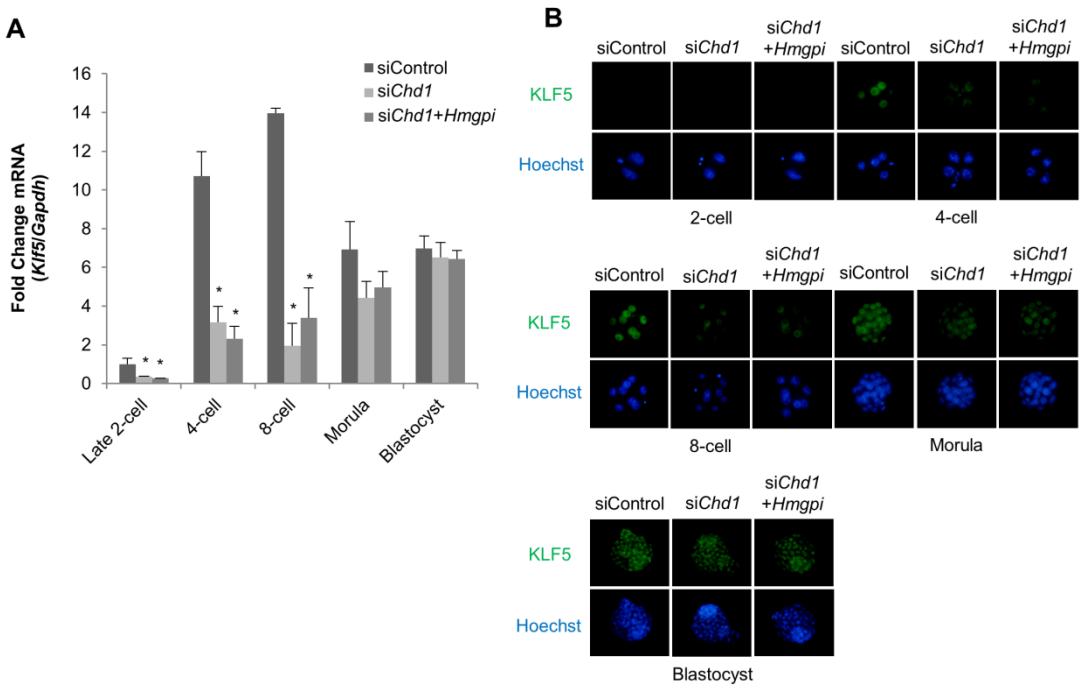

Figure 19. The relationship between *Hmgpi* and *Klf5*.

(A) qRT-PCR of *Klf5* mRNA in control, *Chd1*-knockdown, and *Chd1*-knockdown-*Hmgpi*-rescue embryos from the late 2-cell to the blastocyst stages (*$p < 0.05$). The expression levels were normalized to *Gapdh* as an internal control. The mRNA levels of the late 2-cell control embryos were set to 1. Data are expressed as the mean ± SEM (n = 3). (B) Immunostaining of KLF5 protein in control, *Chd1*-knockdown, and *Chd1*-knockdown-*Hmgpi*-rescue embryos (green, KLF5; blue, chromatin).

Discussion

CHD1, a chromatin remodeling factor, recognizes H3K4me3 (Sims et al, 2005), facilitates the competency of pre-mRNA maturation (Sims et al, 2007), and is required for the maintenance of mouse ES cell pluripotency (Fazzio & Panning, 2010; Gaspar-Maia et al, 2009). CHD1 is also necessary for the incorporation of the variant histone H3.3 in the absence of transcription into paternal pronuclear chromatin at fertilization in *Drosophila* embryos (Konev et al, 2007). Here, we observed the expression pattern of *Chd1* and its protein localization during mouse preimplantation development. We showed that *Chd1*-knockdown leads to embryonic lethality after implantation due to the suppression of zygotic *Oct4* and *Cdx2* expression through the blastocyst stage, suggesting that CHD1 is involved in regulating gene expression that governs cell fate specification and the maintenance of pluripotency.

It has been reported that the maintenance of pluripotency depends on OCT4 functions during preimplantation development (Nichols et al, 1998; Shao et al, 2008). *Oct4*, an ICM marker, is known to negatively interact with *Cdx2*, a TE marker, and both genes are known as key regulators in cell fate specification (Niwa et al, 2005; Ralston et al, 2010; Strumpf et al, 2005). *Oct4* knockout mouse embryos can develop to morphologically normal blastocysts; however, developmental arrest occurs during the postimplantation period due to a loss of pluripotency (Nichols et al, 1998; Ralston et al, 2010). By contrast, *Cdx2* knockout mouse embryos are arrested at the morula stage due to a failure of blastocoel formation (Strumpf et al, 2005). In this study, we observed that *Chd1*-knockdown embryos can also develop to morphologically normal blastocysts but exhibit embryonic lethality due to the suppression of *Oct4* and *Cdx2*. Although *Chd1*-knockdown embryos can develop to morphologically normal blastocysts despite the suppression of *Cdx2*, it is probable that low levels of remaining CDX2 protein may function during trophectoderm development.

It has been reported that the expression of *Oct4* and *Cdx2* at MGA is regulated by *Hmgpi* and *Klf5*, both of which begin to be expressed at ZGA (Ema et al, 2008; Lin et al, 2010; Yamada et al, 2010), suggesting that *Hmgpi* and *Klf5* regulate the initiation of cell fate specification. Several recent studies show that after MGA, the Hippo signaling pathway becomes active and the nuclear accumulation of YAP is inhibited in the inner cells—the future ICM—leading to the expression of *Oct4*. Correspondingly, Hippo signaling is inactive and YAP is accumulated in the nuclei of the outer cells—the future TE—leading to the expression of *Cdx2* (Alarcon, 2010; Cockburn et al, 2013; Hirate et al, 2012; Hirate et al, 2013; Home et al, 2012; Leung & Zernicka-Goetz, 2013; Nishioka et al, 2009; Nishioka et al, 2008; Rayon et al, 2014; Yagi et al, 2007). Additionally, other recent studies showed that after the initiation of cell fate specification, TE-specific genes are silenced in the inner cells via H3K9 methylation by ESET, a histone H3K9 methyltransferase (Yuan et al, 2009); whereas in the outer cells, ICM-specific genes are silenced via H3K9 methylation by SUV39H1, a histone H3K9 methyltransferase (Alder et al, 2010). Altogether, the expression of both *Oct4* and *Cdx2* are under the control of *Hmgpi* and *Klf5* before the initiation of cell fate specification, and after the initiation of cell fate specification the expression of both molecules is regulated comprehensively by HMGPI, KLF5, the Hippo pathway, and epigenetic factors. In the present study, our results showed that in *Chd1*-knockdown embryos, the suppression of *Hmgpi* expression continued until the blastocyst stage. Accordingly, we investigated the effects of *Hmgpi*-rescue in *Chd1*-knockdown embryos on *Oct4* and *Cdx2* expression and postimplantation development. We observed that *Oct4* and *Cdx2* expression, normal ICM-derived colony formation, and the numbers of live offspring were all restored in *Chd1*-knockdown-*Hmgpi*-rescue embryos, suggesting that CHD1 plays important roles as a trigger for both *Oct4* and *Cdx2* expression through the regulation of *Hmgpi* expression at ZGA.

Our results also showed that the suppression of *Klf5* expression was relieved by the morula stage, when *Klf5* expression recovered spontaneously. Furthermore, we showed that the rescue of HMGPI had no effect on *Klf5* expression in *Chd1*-knockdown-*Hmgpi*-rescue embryos, suggesting that there is no direct interaction between *Hmgpi* and *Klf5* during preimplantation development, and that CHD1 regulates the expression of *Klf5* through the 8-cell stage. However, the mechanism regulating the spontaneous recovery of *Klf5* expression in *Chd1*-knockdown embryos after the morula stage is unknown.

It has been reported that the levels of di- and trimethylated H3K4 are important at ZGA in the mouse and that most embryos lacking maternal *Mll2*, an H3K4 methyltransferase, are arrested between the 1- to 4-cell stages due to decreased levels of H3K4me2 and H3K4me3 at ZGA (Andreu-Vieyra et al, 2010a). ZGA is one of the most important events for normal embryo development in the mouse (Li et al, 2010; Minami et al, 2007). In the present study, we demonstrated that CHD1, an H3K4me3-recognizing chromatin-remodeling factor, is involved in the regulation of gene expression at ZGA, and affects cell fate specification and the development of mouse postimplantation embryos.

In conclusion, we demonstrated that CHD1 regulates the initiation of zygotic *Oct4* and *Cdx2* expression at MGA via the activation of *Hmgpi* and *Klf5* expression at ZGA. Thereafter, both HMGPI and KLF5—under the control of CHD1—regulate the expression of *Oct4* and *Cdx2*, and thus, the initiation of cell fate specification. After the initiation of cell fate specification, *Klf5* expression escapes from the control of CHD1, and HMGPI regulates the expression of *Oct4* in the future ICM and the expression of *Cdx2* in the future TE.

Chapter 5

General Discussion

A previous study shows that in oocytes lacking functional *Mll2*, an H3K4 methyltransferase, chromosomes are misaligned, and maturation is arrested due to the decreased the levels of H3K4me2/3, and most embryos lacking maternal *Mll2* are arrested between the 1- to 4-cell stages due to the decreased levels of H3K4me2/3 at ZGA (Andreu-Vieyra et al, 2010a), suggesting that the levels of di- and trimethylated H3K4 are important during oocyte maturation and at ZGA in the mouse. However, the detail molecular mechanisms of H3K4me2/3 are unknown. In the present study, we showed that loss of ING3 function led to symmetric cell division. In *Ing3*-knockdwon oocytes, the disruption of oocyte polarization abrogated spindle migration and led to symmetric cell division during polar body extrusion. It is reported that ING3 is a subunit of the NuA4 histone acetyltransferase complex and bind to H3K4me3 with PHD motif (Doyon et al, 2006; He et al, 2005). The NuA4 histone acetyltransferase complex governs the acetylation of histones H4 and H2A (Doyon & Cote, 2004). In the present study, we demonstrated that ING3 regulated the expression of *mTOR* through promoting H4K12 acetylation in fully grown GV oocytes and the binding of ING3 to the chromatin in fully grown GV oocytes, suggesting that ING3 functions as a chromatin remodeling factor and is involved in asymmetric cell division during oocyte maturation.

In the present study, we also showed that loss of SMYD3 or CHD1 function led to embryonic lethality after implantation. *Smyd3*-knockdown reduced the expression of ICM/EPI markers, e.g., *Oct4*, *Nanog*, and *Sox2*; of PE markers, e.g., *Gata6*; and of TE markers, e.g., *Cdx2* and *Eomes* at the blastocyst stage. Especially, the expressions of *Oct4* and *Cdx2* were reduced from MGA. However, in *Smyd3*-knockdown embryos global H3K4me3 levels appeared

unchanged. Previous studies showed that MLL2, one of the H3K4 methyltransferases, affects the global H3K4me3 levels at ZGA (Andreu-Vieyra et al), and the SETD1A/SETD1B methyltransferase complex that modifies H3K4 affects the global H3K4me3 levels at MGA (Bi et al). Additionally, previous studies demonstrated that *Smyd3*-knockdown leads to the selective decrease in H3K4 methylation levels on oncogene promoter regions in cancer cells (Cock-Rada et al; Liu et al; Medjkane et al). From these observations it is possible that H3K4me3 level depends on the type of methyltransferase and that SMYD3 modified H3K4 within the promoter regions of the lineage-specific genes. *Chd1*-knockdown also reduced the expression of *Oct4* and *Cdx2* from MGA. Additionally, *Chd1*-knockdown reduced the expressions of *Hmgpi* and *Klf5* at ZGA. With respect to *Hmgpi*, the suppression of *Hmgpi* expression continued until the blastocyst stage in *Chd1*-knockdown embryos. On the other hand, *Klf5* expression was suppressed at the 4- and 8-cell stages; however, the expression gradually recovered after the morula stage in *Chd1*-knockdown embryos. Accordingly, we investigated the effects of *Hmgpi*-rescue in *Chd1*-knockdown embryos on *Oct4* and *Cdx2* expression and postimplantation development. We observed that *Oct4* and *Cdx2* expression, normal ICM-derived colony formation, and the numbers of live offspring were all restored in *Chd1*-knockdown-*Hmgpi*-rescue embryos, suggesting that CHD1 plays important roles as a trigger for both *Oct4* and *Cdx2* expression through the regulation of *Hmgpi* expression at ZGA. Phenotype of *Smyd3*-knockdown and *Chd1*-knockdown is very similar. Therefore, we hypothesized that SMYD3 modified H3K4 within the promoter regions of the lineage-specific genes, and then CHD1 recognized the H3K4me3, resulting in transcriptional activation.

In conclusion, our results indicated the possibility that an elucidation of the epigenetic factors which are involved in H3K4me3 may shed light on the molecular mechanisms of oocyte maturation and ZGA in mouse.

Acknowledgements

I wish to express my sincere thank to Associated Professor Naojiro Minami for helpful advice on the occasion of completion of this study.

I also thank to Professor Hiroshi Imai, Associated Professor Masayasu Yamada, Dr. Kaneko (Graduate School of Medicine, Kyoto University), and Dr. Satoshi Tsukamoto (National Institute of Radiological Sciences) for helpful advice and technical assistance.

References

Abdalla H, Yoshizawa Y, Hochi S (2009) Active demethylation of paternal genome in mammalian zygotes. *J Reprod Dev* **55:** 356-360

Aguissa-Toure A-H, Wong RPC, Li G (2011) The ING family tumor suppressors: from structure to function. *Cellular and Molecular Life Sciences* **68:** 45-54

Akiyama T, Suzuki O, Matsuda J, Aoki F (2011) Dynamic replacement of histone H3 variants reprograms epigenetic marks in early mouse embryos. *PLoS Genet* **7:** e1002279

Alarcon VB (2010) Cell polarity regulator PARD6B is essential for trophectoderm formation in the preimplantation mouse embryo. *Biol Reprod* **83:** 347-358

Albert M, Helin K (2010) Histone methyltransferases in cancer. *Seminars in Cell & Developmental Biology* **21:** 209-220

Albert M, Peters AH (2009) Genetic and epigenetic control of early mouse development. *Curr Opin Genet Dev* **19:** 113-121

Alder O, Lavial F, Helness A, Brookes E, Pinho S, Chandrashekran A, Arnaud P, Pombo A, O'Neill L, Azuara V (2010) Ring1B and Suv39h1 delineate distinct chromatin states at bivalent genes during early mouse lineage commitment. *Development* **137:** 2483-2492

Alexandre H, Mulnard J (1988) Time-lapse cinematography study of the germinal vesicle behaviour in mouse primary oocytes treated with activators of protein kinases A and C. *Gamete Res* **21:** 359-365

Andreu-Vieyra CV, Chen R, Agno JE, Glaser S, Anastassiadis K, Stewart AF, Matzuk MM (2010a) MLL2 is required in oocytes for bulk histone 3 lysine 4 trimethylation and transcriptional silencing. *PLoS Biol* **8**

Andreu-Vieyra CV, Chen R, Agno JE, Glaser S, Anastassiadis K, Stewart AF, Matzuk MM

(2010b) MLL2 Is Required in Oocytes for Bulk Histone 3 Lysine 4 Trimethylation and Transcriptional Silencing. *Plos Biology* **8**

Avilion AA, Nicolis SK, Pevny LH, Perez L, Vivian N, Lovell-Badge R (2003) Multipotent cell lineages in early mouse development depend on SOX2 function. *Genes Dev* **17:** 126-140

Awe JP, Byrne JA (2013) Identifying Candidate Oocyte Reprogramming Factors Using Cross-Species Global Transcriptional Analysis. *Cell Reprogram*

Azoury J, Verlhac M-H, Dumont J (2009) Actin filaments: key players in the control of asymmetric divisions in mouse oocytes. *Biology of the Cell* **101:** 69-76

Bi Y, Lv Z, Wang Y, Hai T, Huo R, Zhou Z, Zhou Q, Sha J (2011) WDR82, a key epigenetics-related factor, plays a crucial role in normal early embryonic development in mice. *Biol Reprod* **84:** 756-764

Burton A, Torres-Padilla ME (2010) Epigenetic reprogramming and development: a unique heterochromatin organization in the preimplantation mouse embryo. *Brief Funct Genomics* **9:** 444-454

Chazaud C, Yamanaka Y, Pawson T, Rossant J (2006) Early lineage segregation between epiblast and primitive endoderm in mouse blastocysts through the Grb2-MAPK pathway. *Dev Cell* **10:** 615-624

Chew JL, Loh YH, Zhang W, Chen X, Tam WL, Yeap LS, Li P, Ang YS, Lim B, Robson P, Ng HH (2005) Reciprocal transcriptional regulation of Pou5f1 and Sox2 via the Oct4/Sox2 complex in embryonic stem cells. *Mol Cell Biol* **25:** 6031-6046

Cock-Rada AM, Medjkane S, Janski N, Yousfi N, Perichon M, Chaussepied M, Chluba J, Langsley G, Weitzman JB (2012) SMYD3 promotes cancer invasion by epigenetic upregulation of the metalloproteinase MMP-9. *Cancer Res* **72:** 810-820

Cockburn K, Biechele S, Garner J, Rossant J (2013) The Hippo pathway member Nf2 is

required for inner cell mass specification. *Curr Biol* **23:** 1195-1201

Coles AH, Jones SN (2009) The ING Gene Family in the Regulation of Cell Growth and Tumorigenesis. *Journal of Cellular Physiology* **218:** 45-57

Corry GN, Tanasijevic B, Barry ER, Krueger W, Rasmussen TP (2009) Epigenetic regulatory mechanisms during preimplantation development. *Birth Defects Res C Embryo Today* **87:** 297-313

Deng MQ, Kishikawa H, Yanagimachi R, Kopf GS, Schultz RM, Williams CJ (2003) Chromatin-mediated cortical granule redistribution is responsible for the formation of the cortical granule-free domain in mouse eggs. *Developmental Biology* **257**

Do DV, Ueda J, Messerschmidt DM, Lorthongpanich C, Zhou Y, Feng B, Guo G, Lin PJ, Hossain MZ, Zhang W, Moh A, Wu Q, Robson P, Ng HH, Poellinger L, Knowles BB, Solter D, Fu XY (2013) A genetic and developmental pathway from STAT3 to the OCT4-NANOG circuit is essential for maintenance of ICM lineages in vivo. *Genes Dev* **27:** 1378-1390

Doyon Y, Cayrou C, Ullah M, Landry AJ, Cote V, Selleck W, Lane WS, Tan S, Yang XJ, Cote J (2006) ING tumor suppressor proteins are critical regulators of chromatin acetylation required for genome expression and perpetuation. *Molecular Cell* **21:** 51-64

Doyon Y, Cote J (2004) The highly conserved and multifunctional NuA4 HAT complex. *Current Opinion in Genetics & Development* **14**

Dumont J, Million K, Sunderland K, Rassinier P, Lim H, Leader B, Verlhac MH (2007) Formin-2 is required for spindle migration and for the late steps of cytokinesis in mouse oocytes. *Dev Biol* **301:** 254-265

Elling U, Klasen C, Eisenberger T, Anlag K, Treier M (2006) Murine inner cell mass-derived lineages depend on Sall4 function. *Proc Natl Acad Sci U S A* **103:** 16319-16324

Ema M, Mori D, Niwa H, Hasegawa Y, Yamanaka Y, Hitoshi S, Mimura J, Kawabe Y, Hosoya T,

Morita M, Shimosato D, Uchida K, Suzuki N, Yanagisawa J, Sogawa K, Rossant J, Yamamoto M, Takahashi S, Fujii-Kuriyama Y (2008) Kruppel-like factor 5 is essential for blastocyst development and the normal self-renewal of mouse ESCs. *Cell Stem Cell* **3:** 555-567

Fazzio TG, Panning B (2010) Control of embryonic stem cell identity by nucleosome remodeling enzymes. *Curr Opin Genet Dev* **20:** 500-504

Fededa JP, Gerlich DW (2012) Molecular control of animal cell cytokinesis. *Nature Cell Biology* **14:** 440-447

Feng Q, Wang H, Ng HH, Erdjument-Bromage H, Tempst P, Struhl K, Zhang Y (2002) Methylation of H3-lysine 79 is mediated by a new family of HMTases without a SET domain. *Curr Biol* **12:** 1052-1058

Frankenberg S, Gerbe F, Bessonnard S, Belville C, Pouchin P, Bardot O, Chazaud C (2011) Primitive endoderm differentiates via a three-step mechanism involving Nanog and RTK signaling. *Dev Cell* **21:** 1005-1013

Fujii T, Tsunesumi S, Yamaguchi K, Watanabe S, Furukawa Y (2011) Smyd3 is required for the development of cardiac and skeletal muscle in zebrafish. *PLoS One* **6:** e23491

Gaspar-Maia A, Alajem A, Polesso F, Sridharan R, Mason MJ, Heidersbach A, Ramalho-Santos J, McManus MT, Plath K, Meshorer E, Ramalho-Santos M (2009) Chd1 regulates open chromatin and pluripotency of embryonic stem cells. *Nature* **460:** 863-U897

Gustafsson MG (2005) Nonlinear structured-illumination microscopy: wide-field fluorescence imaging with theoretically unlimited resolution. *Proc Natl Acad Sci U S A* **102:** 13081-13086

Hamamoto R, Furukawa Y, Morita M, Iimura Y, Silva FP, Li M, Yagyu R, Nakamura Y (2004) SMYD3 encodes a histone methyltransferase involved in the proliferation of cancer cells. *Nat Cell Biol* **6:** 731-740

Hamamoto R, Silva FP, Tsuge M, Nishidate T, Katagiri T, Nakamura Y, Furukawa Y (2006)

Enhanced SMYD3 expression is essential for the growth of breast cancer cells. *Cancer Sci* **97:** 113-118

Hamatani T, Carter MG, Sharov AA, Ko MS (2004) Dynamics of global gene expression changes during mouse preimplantation development. *Dev Cell* **6:** 117-131

Hatanaka Y, Shimizu N, Nishikawa S, Tokoro M, Shin SW, Nishihara T, Amano T, Anzai M, Kato H, Mitani T, Hosoi Y, Kishigami S, Matsumoto K (2013) GSE is a maternal factor involved in active DNA demethylation in zygotes. *PLoS One* **8:** e60205

He GHY, Helbing CC, Wagner MJ, Sensen CW, Riabowol K (2005) Phylogenetic analysis of the ING family of PHD finger proteins. *Molecular Biology and Evolution* **22:** 104-116

Hirasawa R, Chiba H, Kaneda M, Tajima S, Li E, Jaenisch R, Sasaki H (2008) Maternal and zygotic Dnmt1 are necessary and sufficient for the maintenance of DNA methylation imprints during preimplantation development. *Genes Dev* **22:** 1607-1616

Hirate Y, Cockburn K, Rossant J, Sasaki H (2012) Tead4 is constitutively nuclear, while nuclear vs. cytoplasmic Yap distribution is regulated in preimplantation mouse embryos. In *Proc Natl Acad Sci U S A* Vol. 109, pp E3389-3390; author reply E3391-3382. United States

Hirate Y, Hirahara S, Inoue K, Suzuki A, Alarcon VB, Akimoto K, Hirai T, Hara T, Adachi M, Chida K, Ohno S, Marikawa Y, Nakao K, Shimono A, Sasaki H (2013) Polarity-dependent distribution of angiomotin localizes Hippo signaling in preimplantation embryos. *Curr Biol* **23:** 1181-1194

Ho Y, Wigglesworth K, Eppig JJ, Schultz RM (1995) Preimplantation development of mouse embryos in KSOM: augmentation by amino acids and analysis of gene expression. *Mol Reprod Dev* **41:** 232-238

Home P, Saha B, Ray S, Dutta D, Gunewardena S, Yoo B, Pal A, Vivian JL, Larson M, Petroff M, Gallagher PG, Schulz VP, White KL, Golos TG, Behr B, Paul S (2012) Altered subcellular

localization of transcription factor TEAD4 regulates first mammalian cell lineage commitment. *Proc Natl Acad Sci U S A* **109:** 7362-7367

Hosny NA, Song M, Connelly JT, Ameer-Beg S, Knight MM, Wheeler AP (2013) Super-resolution imaging strategies for cell biologists using a spinning disk microscope. *PLoS One* **8:** e74604

Huang X, Ding L, Pan R, Ma PF, Cheng PP, Zhang CH, Shen YT, Xu L, Liu Y, He XQ, Qi ZQ, Wang HL (2013) WHAMM is required for meiotic spindle migration and asymmetric cytokinesis in mouse oocytes. *Histochem Cell Biol* **139:** 525-534

Iden S, Collard JG (2008) Crosstalk between small GTPases and polarity proteins in cell polarization. *Nature Reviews Molecular Cell Biology* **9:** 846-859

Isaji Y, Murata M, Takaguchi N, Mukai T, Tajima Y, Imai H, Yamada M (2013) Valproic acid treatment from the 4-cell stage improves Oct4 expression and nuclear distribution of histone H3K27me3 in mouse cloned blastocysts. *J Reprod Dev* **59:** 196-204

Jafarnejad SM, Li G (2012) Regulation of p53 by ING family members in suppression of tumor initiation and progression. *Cancer and Metastasis Reviews* **31:** 55-73

Jordan SN, Canman JC (2012) Rho GTPases in Animal Cell Cytokinesis: An Occupation by the One Percent. *Cytoskeleton* **69:** 919-930

Kageyama S-i, Liu H, Kaneko N, Ooga M, Nagata M, Aoki F (2007) Alterations in epigenetic modifications during oocyte growth in mice. *Reproduction* **133:** 85-94

Kang M, Piliszek A, Artus J, Hadjantonakis AK (2013) FGF4 is required for lineage restriction and salt-and-pepper distribution of primitive endoderm factors but not their initial expression in the mouse. *Development* **140:** 267-279

Kidder BL, Palmer S, Knott JG (2009) SWI/SNF-Brg1 regulates self-renewal and occupies core pluripotency-related genes in embryonic stem cells. *Stem Cells* **27:** 317-328

Konev AY, Tribus M, Park SY, Podhraski V, Lim CY, Emelyanov AV, Vershilova E, Pirrotta V, Kadonaga JT, Lusser A, Fyodorov DV (2007) CHD1 motor protein is required for deposition of histone variant H3.3 into chromatin in vivo. *Science* **317:** 1087-1090

Kubiak J, Paldi A, Weber M, Maro B (1991) Genetically identical parthenogenetic mouse embryos produced by inhibition of the first meiotic cleavage with cytochalasin D. *Development* **111:** 763-769

Latham KE, Schultz RM (2001) Embryonic genome activation. *Front Biosci* **6:** D748-759

Lee SE, Sun SC, Choi HY, Uhm SJ, Kim NH (2012) mTOR is required for asymmetric division through small GTPases in mouse oocytes. *Mol Reprod Dev* **79:** 356-366

Lepikhov K, Walter J (2004) Differential dynamics of histone H3 methylation at positions K4 and K9 in the mouse zygote. *BMC Dev Biol* **4:** 12

Leung CY, Zernicka-Goetz M (2013) Angiomotin prevents pluripotent lineage differentiation in mouse embryos via Hippo pathway-dependent and -independent mechanisms. *Nat Commun* **4:** 2251

Levey IL, Troike DE, Brinster RL (1977) Effects of alpha-amanitin on the development of mouse ova in culture. *J Reprod Fertil* **50:** 147-150

Li L, Zheng P, Dean J (2010) Maternal control of early mouse development. *Development* **137:** 859-870

Lin SC, Wani MA, Whitsett JA, Wells JM (2010) Klf5 regulates lineage formation in the pre-implantation mouse embryo. *Development* **137:** 3953-3963

Liu C, Fang X, Ge Z, Jalink M, Kyo S, Björkholm M, Gruber A, Sjöberg J, Xu D (2007) The telomerase reverse transcriptase (hTERT) gene is a direct target of the histone methyltransferase SMYD3. *Cancer Res* **67:** 2626-2631

Liu C, Wang C, Wang K, Liu L, Shen Q, Yan K, Sun X, Chen J, Liu J, Ren H, Liu H, Xu Z, Hu

S, Xu D, Fan Y (2013) SMYD3 as an oncogenic driver in prostate cancer by stimulation of androgen receptor transcription. *J Natl Cancer Inst* **105:** 1719-1728

Livak KJ, Schmittgen TD (2001) Analysis of relative gene expression data using real-time quantitative PCR and the 2(-Delta Delta C(T)) Method. In *Methods* Vol. 25, pp 402-408. United States: 2001 Elsevier Science (USA).

Longo FJ, Chen DY (1985) Development of cortical polarity in mouse eggs: involvement of the meiotic apparatus. In *Dev Biol* Vol. 107, pp 382-394. United States

Lu M, Chen F, Wang Q, Wang K, Pan Q, Zhang X (2012) Downregulation of inhibitor of growth 3 is correlated with tumorigenesis and progression of hepatocellular carcinoma. *Oncology Letters* **4**

Ma P, Schultz RM (2013) Histone Deacetylase 2 (HDAC2) Regulates Chromosome Segregation and Kinetochore Function via H4K16 Deacetylation during Oocyte Maturation in Mouse. In *PLoS Genet* Vol. 9, p e1003377. United States

Maro B, Verlhac MH (2002) Polar body formation: new rules for asymmetric divisions. *Nature Cell Biology* **4**

Medjkane S, Cock-Rada A, Weitzman JB (2012) Role of the SMYD3 histone methyltransferase in tumorigenesis: local or global effects? In *Cell Cycle* Vol. 11, p 1865. United States

Mellor J (2006) It takes a PHD to read the histone code. *Cell* **126:** 22-24

Metchat A, Akerfelt M, Bierkamp C, Delsinne V, Sistonen L, Alexandre H, Christians ES (2009) Mammalian Heat Shock Factor 1 Is Essential for Oocyte Meiosis and Directly Regulates Hsp90 alpha Expression. *Journal of Biological Chemistry* **284:** 9521-9528

Miao YL, Kikuchi K, Sun QY, Schatten H (2009) Oocyte aging: cellular and molecular changes, developmental potential and reversal possibility. In *Hum Reprod Update* Vol. 15, pp 573-585. England

Minami N, Sasaki K, Aizawa A, Miyamoto M, Imai H (2001) Analysis of gene expression in mouse 2-cell embryos using fluorescein differential display: comparison of culture environments. *Biol Reprod* **64:** 30-35

Minami N, Suzuki T, Tsukamoto S (2007) Zygotic gene activation and maternal factors in mammals. *J Reprod Dev* **53:** 707-715

Mitsui K, Tokuzawa Y, Itoh H, Segawa K, Murakami M, Takahashi K, Maruyama M, Maeda M, Yamanaka S (2003) The homeoprotein Nanog is required for maintenance of pluripotency in mouse epiblast and ES cells. *Cell* **113:** 631-642

Morgan HD, Santos F, Green K, Dean W, Reik W (2005) Epigenetic reprogramming in mammals. *Hum Mol Genet* **14 Spec No 1:** R47-58

Morris SA, Teo RT, Li H, Robson P, Glover DM, Zernicka-Goetz M (2010) Origin and formation of the first two distinct cell types of the inner cell mass in the mouse embryo. *Proc Natl Acad Sci U S A* **107:** 6364-6369

Nagashima M, Shiseki M, Pedeux RM, Okamura S, Kitahama-Shiseki M, Miura K, Yokota J, Harris CC (2003) A novel PHD-finger motif protein, p47ING3, modulates p53-mediated transcription, cell cycle control, and apoptosis. *Oncogene* **22:** 343-350

Nakamura T, Liu YJ, Nakashima H, Umehara H, Inoue K, Matoba S, Tachibana M, Ogura A, Shinkai Y, Nakano T (2012) PGC7 binds histone H3K9me2 to protect against conversion of 5mC to 5hmC in early embryos. *Nature* **486:** 415-419

Nichols J, Zevnik B, Anastassiadis K, Niwa H, Klewe-Nebenius D, Chambers I, Scholer H, Smith A (1998) Formation of pluripotent stem cells in the mammalian embryo depends on the POU transcription factor Oct4. *Cell* **95:** 379-391

Nishioka N, Inoue K, Adachi K, Kiyonari H, Ota M, Ralston A, Yabuta N, Hirahara S, Stephenson RO, Ogonuki N, Makita R, Kurihara H, Morin-Kensicki EM, Nojima H, Rossant J,

Nakao K, Niwa H, Sasaki H (2009) The Hippo signaling pathway components Lats and Yap pattern Tead4 activity to distinguish mouse trophectoderm from inner cell mass. *Dev Cell* **16:** 398-410

Nishioka N, Yamamoto S, Kiyonari H, Sato H, Sawada A, Ota M, Nakao K, Sasaki H (2008) Tead4 is required for specification of trophectoderm in pre-implantation mouse embryos. *Mech Dev* **125:** 270-283

Niwa H, Toyooka Y, Shimosato D, Strumpf D, Takahashi K, Yagi R, Rossant J (2005) Interaction between Oct3/4 and Cdx2 determines trophectoderm differentiation. *Cell* **123:** 917-929

Nowak SJ, Corces VG (2004) Phosphorylation of histone H3: a balancing act between chromosome condensation and transcriptional activation. *Trends Genet* **20:** 214-220

Okumura-Nakanishi S, Saito M, Niwa H, Ishikawa F (2005) Oct-3/4 and Sox2 regulate Oct-3/4 gene in embryonic stem cells. *J Biol Chem* **280:** 5307-5317

Pollard TD (2007) Regulation of actin filament assembly by Arp2/3 complex and formins. *Annual Review of Biophysics and Biomolecular Structure* **36:** 451-477

Ralston A, Cox BJ, Nishioka N, Sasaki H, Chea E, Rugg-Gunn P, Guo G, Robson P, Draper JS, Rossant J (2010) Gata3 regulates trophoblast development downstream of Tead4 and in parallel to Cdx2. *Development* **137:** 395-403

Rasmussen TP, Corry GN (2010) Epigenetic pre-patterning and dynamics during initial stages of mammalian preimplantation development. *J Cell Physiol* **225:** 333-336

Rayon T, Menchero S, Nieto A, Xenopoulos P, Crespo M, Cockburn K, Canon S, Sasaki H, Hadjantonakis AK, de la Pompa JL, Rossant J, Manzanares M (2014) Notch and hippo converge on cdx2 to specify the trophectoderm lineage in the mouse blastocyst. *Dev Cell* **30:** 410-422

Rodda DJ, Chew JL, Lim LH, Loh YH, Wang B, Ng HH, Robson P (2005) Transcriptional

regulation of nanog by OCT4 and SOX2. *J Biol Chem* **280:** 24731-24737

Rossant J (2004) Lineage development and polar asymmetries in the peri-implantation mouse blastocyst. *Semin Cell Dev Biol* **15:** 573-581

Russ AP, Wattler S, Colledge WH, Aparicio SA, Carlton MB, Pearce JJ, Barton SC, Surani MA, Ryan K, Nehls MC, Wilson V, Evans MJ (2000) Eomesodermin is required for mouse trophoblast development and mesoderm formation. *Nature* **404:** 95-99

Santos F, Peters AH, Otte AP, Reik W, Dean W (2005) Dynamic chromatin modifications characterise the first cell cycle in mouse embryos. *Dev Biol* **280:** 225-236

Sarmento OF, Digilio LC, Wang Y, Perlin J, Herr JC, Allis CD, Coonrod SA (2004) Dynamic alterations of specific histone modifications during early murine development. *J Cell Sci* **117:** 4449-4459

Schrode N, Saiz N, Di Talia S, Hadjantonakis AK (2014) GATA6 levels modulate primitive endoderm cell fate choice and timing in the mouse blastocyst. *Dev Cell* **29:** 454-467

Schultz RM (1993) Regulation of zygotic gene activation in the mouse. *Bioessays* **15:** 531-538

Schultz RM, Worrad DM (1995) Role of chromatin structure in zygotic gene activation in the mammalian embryo. *Semin Cell Biol* **6:** 201-208

Shao GB, Ding HM, Gong AH (2008) Role of histone methylation in zygotic genome activation in the preimplantation mouse embryo. *In Vitro Cell Dev Biol Anim* **44:** 115-120

Shi L, Wu J (2009) Epigenetic regulation in mammalian preimplantation embryo development. *Reprod Biol Endocrinol* **7:** 59

Shilatifard A (2006) Chromatin modifications by methylation and ubiquitination: implications in the regulation of gene expression. *Annu Rev Biochem* **75:** 243-269

Shindo T, Manabe I, Fukushima Y, Tobe K, Aizawa K, Miyamoto S, Kawai-Kowase K, Moriyama N, Imai Y, Kawakami H, Nishimatsu H, Ishikawa T, Suzuki T, Morita H, Maemura K,

Sata M, Hirata Y, Komukai M, Kagechika H, Kadowaki T, Kurabayashi M, Nagai R (2002) Kruppel-like zinc-finger transcription factor KLF5/BTEB2 is a target for angiotensin II signaling and an essential regulator of cardiovascular remodeling. *Nat Med* **8:** 856-863

Simic R, Lindstrom DL, Tran HG, Roinick KL, Costa PJ, Johnson AD, Hartzog GA, Arndt KM (2003) Chromatin remodeling protein Chd1 interacts with transcription elongation factors and localizes to transcribed genes. *Embo j* **22:** 1846-1856

Sims RJ, 3rd, Chen CF, Santos-Rosa H, Kouzarides T, Patel SS, Reinberg D (2005) Human but not yeast CHD1 binds directly and selectively to histone H3 methylated at lysine 4 via its tandem chromodomains. *J Biol Chem* **280:** 41789-41792

Sims RJ, 3rd, Millhouse S, Chen CF, Lewis BA, Erdjument-Bromage H, Tempst P, Manley JL, Reinberg D (2007) Recognition of trimethylated histone H3 lysine 4 facilitates the recruitment of transcription postinitiation factors and pre-mRNA splicing. *Mol Cell* **28:** 665-676

Sterner DE, Berger SL (2000) Acetylation of histones and transcription-related factors. *Microbiol Mol Biol Rev* **64:** 435-459

Stokes DG, Tartof KD, Perry RP (1996) CHD1 is concentrated in interbands and puffed regions of Drosophila polytene chromosomes. *Proc Natl Acad Sci U S A* **93:** 7137-7142

Strumpf D, Mao CA, Yamanaka Y, Ralston A, Chawengsaksophak K, Beck F, Rossant J (2005) Cdx2 is required for correct cell fate specification and differentiation of trophectoderm in the mouse blastocyst. *Development* **132:** 2093-2102

Sun QY, Schatten H (2006) Regulation of dynamic events by microfilaments during oocyte maturation and fertilization. *Reproduction* **131:** 193-205

Sun SC, Gao WW, Xu YN, Jin YX, Wang QL, Yin XJ, Cui XS, Kim NH (2012) Degradation of actin nucleators affects cortical polarity of aged mouse oocytes. *Fertility and Sterility* **97:** 984-990

Sun SC, Sun QY, Kim NH (2011a) JMY is required for asymmetric division and cytokinesis in mouse oocytes. *Molecular Human Reproduction* **17:** 296-304

Sun SC, Wang ZB, Xu YN, Lee SE, Cui XS, Kim NH (2011b) Arp2/3 complex regulates asymmetric division and cytokinesis in mouse oocytes. *PLoS One* **6:** e18392

Suzuki S, Nozawa Y, Tsukamoto S, Kaneko T, Imai H, Minami N (2013) ING3 Is Essential for Asymmetric Cell Division during Mouse Oocyte Maturation. *PLoS One* **8:** e74749

Tsukamoto S, Hara T, Yamamoto A, Ohta Y, Wada A, Ishida Y, Kito S, Nishikawa T, Minami N, Sato K, Kokubo T (2013) Functional analysis of lysosomes during mouse preimplantation embryo development. *J Reprod Dev* **59:** 33-39

Van Aller GS, Reynoird N, Barbash O, Huddleston M, Liu S, Zmoos AF, McDevitt P, Sinnamon R, Le B, Mas G, Annan R, Sage J, Garcia BA, Tummino PJ, Gozani O, Kruger RG (2012) Smyd3 regulates cancer cell phenotypes and catalyzes histone H4 lysine 5 methylation. *Epigenetics* **7:** 340-343

Van Blerkom J, Bell H (1986) Regulation of development in the fully grown mouse oocyte: chromosome-mediated temporal and spatial differentiation of the cytoplasm and plasma membrane. *J Embryol Exp Morphol* **93:** 213-238

Verlhac MH, Lefebvre C, Guillaud P, Rassinier P, Maro B (2000) Asymmetric division in mouse oocytes: with or without Mos. *Curr Biol* **10:** 1303-1306

Wang H, Dey SK (2006) Roadmap to embryo implantation: clues from mouse models. *Nat Rev Genet* **7:** 185-199

Wang K, Sengupta S, Magnani L, Wilson CA, Henry RW, Knott JG (2010) Brg1 is required for Cdx2-mediated repression of Oct4 expression in mouse blastocysts. *PLoS One* **5:** e10622

Wang S, Hu J, Guo X, Liu JX, Gao S (2009) ADP-Ribosylation Factor 1 Regulates Asymmetric Cell Division in Female Meiosis in the Mouse. *Biology of Reproduction* **80:** 555-562

Wang YM, Li G (2006) ING3 promotes UV-induced apoptosis via Fas/caspase-8 pathway in melanoma cells. *Journal of Biological Chemistry* **281:** 11887-11893

Warner CM, Versteegh LR (1974) In vivo and in vitro effect of alpha-amanitin on preimplantation mouse embryo RNA polymerase. *Nature* **248:** 678-680

Webb M, Howlett SK, Maro B (1986) Parthenogenesis and cytoskeletal organization in ageing mouse eggs. *J Embryol Exp Morphol* **95:** 131-145

Woodage T, Basrai MA, Baxevanis AD, Hieter P, Collins FS (1997) Characterization of the CHD family of proteins. *Proc Natl Acad Sci U S A* **94:** 11472-11477

Wullschleger S, Loewith R, Hall MN (2006) TOR signaling in growth and metabolism. *Cell* **124:** 471-484

Xu JY, Chen LB, Yang Z, Wei HY, Xu RH (2006) [Inhibition of SMYD3 gene expression by RNA interference induces apoptosis in human hepatocellular carcinoma cell line HepG2]. *Ai Zheng* **25:** 526-532

Yagi R, Kohn MJ, Karavanova I, Kaneko KJ, Vullhorst D, DePamphilis ML, Buonanno A (2007) Transcription factor TEAD4 specifies the trophectoderm lineage at the beginning of mammalian development. *Development* **134:** 3827-3836

Yamada M, Hamatani T, Akutsu H, Chikazawa N, Kuji N, Yoshimura Y, Umezawa A (2010) Involvement of a novel preimplantation-specific gene encoding the high mobility group box protein Hmgpi in early embryonic development. *Hum Mol Genet* **19:** 480-493

Yoshikawa T, Piao Y, Zhong J, Matoba R, Carter MG, Wang Y, Goldberg I, Ko MS (2006) High-throughput screen for genes predominantly expressed in the ICM of mouse blastocysts by whole mount in situ hybridization. *Gene Expr Patterns* **6:** 213-224

Yuan P, Han J, Guo G, Orlov YL, Huss M, Loh YH, Yaw LP, Robson P, Lim B, Ng HH (2009) Eset partners with Oct4 to restrict extraembryonic trophoblast lineage potential in embryonic

stem cells. *Genes Dev* **23:** 2507-2520

Zhang CH, Wang ZB, Quan S, Huang X, Tong JS, Ma JY, Guo L, Wei YC, Ouyang YC, Hou Y, Xing FQ, Sun QY (2011) GM130, a cis-Golgi protein, regulates meiotic spindle assembly and asymmetric division in mouse oocyte. *Cell Cycle* **10:** 1861-1870

Zhang J, Tam WL, Tong GQ, Wu Q, Chan HY, Soh BS, Lou Y, Yang J, Ma Y, Chai L, Ng HH, Lufkin T, Robson P, Lim B (2006) Sall4 modulates embryonic stem cell pluripotency and early embryonic development by the transcriptional regulation of Pou5f1. *Nat Cell Biol* **8:** 1114-1123

Zhang K, Dai X, Wallingford MC, Mager J (2013) Depletion of Suds3 reveals an essential role in early lineage specification. *Dev Biol* **373:** 359-372

Zhang Y, Reinberg D (2001) Transcription regulation by histone methylation: interplay between different covalent modifications of the core histone tails. *Genes Dev* **15:** 2343-2360

Zheng P, Baibakov B, Wang XH, Dean J (2012) PtdIns(3,4,5)P3 is constitutively synthesized and required for spindle translocation during meiosis in mouse oocytes. In *J Cell Sci*.

Zhong ZS, Huo LJ, Liang CG, Chen DY, Sun QY (2005) Small GTPase RhoA is required for ooplasmic segregation and spindle rotation, but not for spindle organization and chromosome separation during mouse oocyte maturation, fertilization, and early cleavage. *Mol Reprod Dev* **71:** 256-261

Zou JN, Wang SZ, Yang JS, Luo XG, Xie JH, Xi T (2009) Knockdown of SMYD3 by RNA interference down-regulates c-Met expression and inhibits cells migration and invasion induced by HGF. *Cancer Lett* **280:** 78-85